

1 **Recent Advances in Tree Root Mapping and Assessment using Non-**
2 **Destructive Testing Methods: a Focus on Ground Penetrating Radar**

3

4 Amir M. ALANI¹ and Livia LANTINI¹

5 ¹School of Computing and Engineering, University of West London (UWL), St Mary's
6 Road, Ealing, London W5 5RF, UK

7 e-mail: Amir.Alani@uwl.ac.uk (*Corresponding author); Livia.Lantini@uwl.ac.uk

8

9 **Abstract**

10 This paper provides an overview of the existing literature on the subject of assessment
11 and monitoring of tree roots and their interaction with the soil. An overview of tree root
12 systems architecture is given, and the main issues in terms of health and stability of
13 trees, as well as the impact of trees on the built environment, are discussed. An overview
14 of the main destructive and non-destructive testing (NDT) methods is therefore given.
15 The paper also highlights the lack of available research based outputs in the field of tree
16 roots and soil interaction, as well as of the interconnectivity of tree roots with one
17 another. Additionally, the effectiveness of non-destructive methods is demonstrated, in
18 particular ground penetrating radar, in mapping tree root configurations and their
19 interconnectivity. Furthermore, the paper references recent developments in
20 estimating tree root mass density and health.

21 **Keywords:** assessment of tree roots; destructive testing methods; non-destructive
22 testing methods; ground penetrating radar (GPR); tree root interconnectivity; tree root
23 mass density.

24

25 **1. Introduction**

26 The earliest identified fossil tree, from over 385 million years ago, was found in the New
27 York State, USA in 2007. Trees and plants have always been part of life on planet Earth.
28 The impact of trees and their value to human life and the environment have been
29 discussed in numerous publications for decades, even centuries, as suggested in
30 <https://www.savatree.com/whytrees.html>. In more detail, the value of trees within the
31 context of modern life could be considered under the following areas:

- 32 • Ecological and environmental
- 33 • Community and social
- 34 • Aesthetics
- 35 • Commercial and economic

36 Trees and forests are every society's asset and must be looked after and cherished. The
37 contribution of trees and their importance to environmental sustainability are so vast
38 that they can only be compared to the existence of icebergs and our oceans. Prevention
39 from destruction of trees and plants by cutting them at alarming rate for materialistic
40 reasons (i.e. creating wealth in different shapes and forms) are vital to the preservation
41 of life, both for humans and animals, on the planet Earth.

42 Likewise, safeguarding and having planned health monitoring and assessment of the
43 existing trees and plants are equally important. Within this context, the understanding
44 of the health of tree roots and plants (i.e. growth, architecture and interaction with the
45 soil and other tree roots) are of paramount importance.

46 Appropriately managing and caring for natural heritage is more important than ever
47 today (Innes, 1993), and there is a growing awareness of the need to protect the
48 environment. In particular, the preservation of veteran or ancient trees presents a series
49 of conservation challenges that differ from standard arboricultural practices.

50 Among all the tree organs, roots are of vital importance because they have crucial
51 functions in plants and ecosystems: they provide anchorage, supply soil-borne resources
52 and modify soil properties. However, even if roots account for between 10% and 65% of

53 a tree's total biomass, they typically lie below the soil surface, which in turn has limited
54 our understanding of tree root system development and their interaction with the
55 surrounding environment.

56 Various methods have been used to study the root systems of plants. Such investigations
57 are usually carried out using destructive methods, such as excavation or uprooting.
58 Although these techniques can provide direct measurements of the roots, they are
59 onerous, time-consuming and above all destructive. The damage that these techniques
60 inflict on trees leads to a reduction in the number of measurements which can be carried
61 out in the future, making it impossible to assess the status of the roots during a given
62 period. Also, root systems are often destroyed by these inspection methods, thus
63 becoming susceptible to infections and diseases which can lead to the death of the tree.

64 The use of non-destructive techniques for root inspection and analysis has gained
65 popularity in recent years, as this method can provide information about tree root
66 architecture without harming the tree. It also enables long-term monitoring of tree root
67 systems, as no disturbance is caused to their development by the application of these
68 techniques.

69 In this framework, ground penetrating radar (GPR) is widely acknowledged to be a
70 powerful geophysical non-destructive tool, useful in locating buried objects such as
71 bedrocks, artefacts, utilities infrastructure and objects, voids and sub-surface water
72 levels. Recently, several studies have been carried out about the use of GPR for root
73 detection and mapping, as well as for the estimation of root biomass and diameter. This
74 technique has shown great potential due to the reliability of the results and its ease of
75 use. However, some research has led to contradictory results, due probably to
76 difficulties in surveying a non-homogeneous medium such as the soil-root system. For
77 this reason, gaining comprehensive knowledge about tree root systems is advisable in
78 order to improve the use of GPR in this field and the understanding of achieved results.

79 Hence, this review aims to evaluate state of the art in tree root system investigation,
80 from the beginning to the most recent achievements in the non-destructive techniques
81 field. To this purpose, a brief introduction on tree root system architecture is presented,

82 to broaden the understanding of root growth, development and structure, as well as the
83 root system's dependence on the environment and the characteristics of the soil.
84 Following this, the main concerns regarding roots are defined and discussed, divided
85 into health problems which could affect roots and the damage that roots can cause to
86 the environment. The principal techniques for tree root system investigation are listed
87 and examined, from the destructive methods to the non-destructive techniques. The
88 main achievements and limitations of each method are thus discussed.

89 Finally, a comprehensive review of GPR applications to root detection and root index
90 quantifications is carried out, in a section organised as follows:

- 91 • GPR operating principles and signal processing techniques are outlined;
- 92 • The current state of knowledge about GPR use in tree root systems investigations
93 is reviewed;
- 94 • Limiting factors to root surveys using GPR are outlined;
- 95 • Future perspectives are discussed.

96

97 **2. Tree root systems architecture**

98 Tree roots are responsible for water and mineral uptake, carbohydrate storage and
99 hormonal signalling (Pallardy, 2008), as well as for providing support and anchorage in
100 the ground (Coutts, 1983). Thus, the health of the root system, and as a consequence
101 the health of the tree, is closely linked to the soil conditions (Gregory, 2006).

102 Tree roots are usually composed of complex structures, and they can be divided into
103 two main groups:

- 104 • Woody roots: roots that have gone through secondary growth, resulting in a
105 more rigid structure. Such roots have a structural role, as they are essentially
106 responsible for anchoring the tree in the ground, and their lifespan is perennial
107 (Pallardy, 2008). Wilson (1964) observed that woody roots that are located
108 within one or two meters of the stem, the so-called zone of rapid taper, have
109 different features from the roots that are located beyond this area, as the former
110 often exhibit considerable secondary thickening. If the thickening is along the
111 vertical plane, they are called buttress roots, the presence of which has been
112 associated with soils that offer poor anchorage (Henwood, 1973). Beyond the
113 zone of rapid taper emanates a framework of woody structural roots that gather
114 water and nutrients from long distances to the trunk: their size is often
115 influenced by mechanical stresses such as the wind load (Stoke, 1994).
- 116 • Non-woody roots: also known as fine or absorbing roots, they are responsible
117 for the absorption of water and nutrients (Pallardy, 2008), the synthesis of
118 rooting hormone, root exudation, and symbiosis with soil microorganisms. As
119 the name suggests, they do not undergo secondary thickening, are generally
120 small in diameter (<2 mm) and their lifespan ranges from days to weeks,
121 depending on soil conditions and temperature (Pallardy, 2008).

122 Root architecture is quite complex and varies between and within plant species
123 (Gregory, 2006). As far as rooting depth is concerned, it is influenced not only by the
124 tree species but also by the type and conditions of the soil (Stone & Kalisz, 1991): in fact,
125 the downward penetration of roots can be impeded by soils that are poorly aerated or

126 too dense, and by the presence of rock layers or by low soil temperatures. Stone and
127 Kalisz (1991) carried out an extensive study on tree roots, reviewing the existing
128 literature and performing on-site surveys on a wide variety of tree species,
129 demonstrating that root extent is strictly related to site conditions. Indeed, evidence has
130 been found that many species can reach considerable depths if not limited by soil
131 characteristics. According to Jackson et al. (1996), there can be significant differences in
132 rooting depths, depending on the features of the surrounding environment: rooting
133 profiles are shallowest in boreal forests, temperate grasslands, and tundra, due not only
134 to the convenient characteristics of soil moisture and aeration but also the presence of
135 physical barriers to root vertical growth, such as permafrost in tundras and some boreal
136 forests (Bonan, 1992). On the other hand, root distribution is deeper in deserts and xeric
137 shrublands, as the lack of water and nutrients in the shallow subsurface, together with
138 extreme soil surface temperatures, inhibits root development in the upper soil layers
139 (Nobel, 2003) and forces them to grow deeper. Regardless, there is undoubtedly a
140 tendency for tree roots to be concentrated in the surface soil (Wilson, 1964) (Wang, et
141 al., 2006), as it is usually better aerated and moist, it contains a higher concentration of
142 minerals than the deeper layers. Pallardy (2008) states that root density is often higher
143 in the first 30 cm below the soil surface.

144 On the other hand, root spread seems to be less closely related to soil temperature and
145 characteristics (Strong & La Roi, 1983). The extent of root development seems to rely
146 upon the tree species, but also upon the stand density (Stone & Kalisz, 1991) and the
147 presence of competing species (Shainsky & Radosevich, 1992). Many rules of thumb
148 have been presented for estimating root spread, the most common of which is a relation
149 between root extent and canopy diameter (Tubbs, 1977); however, Stone and Kalisz
150 (1991) reported many examples of a maximum lateral root extent of more than 30m
151 from the trunk, and in some cases more than 50m. This seems to demonstrate that roots
152 tend to explore the largest soil area possible, in order to exploit its resources and provide
153 anchorage and stability. These estimates commonly assume that there are few
154 significant physical impediments to root extent; moreover, not much is known about

155 how different trees compete for water and mineral uptake when root systems come in
156 contact with one another.

157 **3. Main issues**

158 **3.1. Health and stability of the tree**

159 Tree diseases are an integral part of natural ecosystems, as they regulate the
160 development of forests (Hansen & Goheen, 2000). The coexistence of plants and
161 pathogens is therefore necessary for the survival of both. However, human activities
162 have often altered the natural balance, breaking down the geographical barriers that
163 had preserved the ecosystems and allowing the movement of wild species (Richardson,
164 et al., 2001). As a consequence of the increase in the global trade of plants, alien
165 pathogens and fungi have invaded entire regions (Santini, et al., 2012) (Liebhold, et al.,
166 2012), sometimes with devastating consequences, as in the Dutch elm disease (Gibbs,
167 1978) and the chestnut blight (Anagnostakis, 1987) cases. Such diseases not only have
168 severe ecological consequences, but they can also have economic repercussions
169 (Aukema, et al., 2011).

170 Fungal infections are one of the main causes of root disease, as fungi are natural
171 components of forests (Hansen & Goheen, 2000). These typically contaminate trees
172 which have already been weakened by other factors, such as other pests or climatic
173 changes (Williams, et al., 1986), and they usually spread from the roots of dead or
174 uprooted trees (Rishbeth, 1972). Fungi penetrate the bark and initiate decay in roots,
175 inducing root rot and infecting coarse roots and the lower stems of trees (Figure 1).



176

177 **Figure 1: Roots and lower stem of a tree infected by *Armillaria root rot* fungi (Canadian Forest Service, 2015)**

178 Plants can live for a long time even if sick, as they continue to collect water and nutrients
179 from healthy roots. Within this time, the infection can spread to other trees through
180 root contact (Hansen & Goheen, 2000). Eventually, rotten roots will not be able to
181 provide anchorage and sustenance, and the contaminated tree will die either by wind-
182 throw or disease (Rishbeth, 1972).

183 The recognition of root diseases is difficult, as fungal infections do not show visible
184 symptoms. Manifestations of diseases can include the production of mushrooms around
185 the tree base, foliage discolouration and reduced growth (Williams, et al., 1986).

186 However, these symptoms can take several years to materialise if the tree is large or old,
187 and by the time the disease is recognised, it is often too late for any interventions.

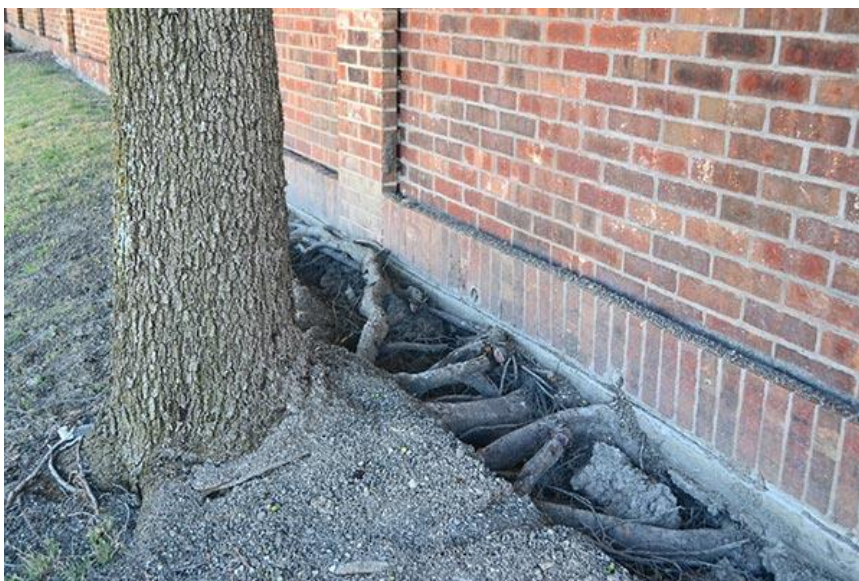
188

189 **3.2. Built environment**

190 **3.2.1. Buildings**

191 Despite being an essential presence in urban and archaeological sites, trees can also
192 cause damage to structures and buildings. Damage can occur through direct contact
193 with tree roots (Satriani, et al., 2010), as their growth can cause structures to uplift. This
194 is more likely to take place near the tree trunk, as the pressure exerted by roots
195 decreases rapidly with distance (MacLeod & Cram, 1996). This usually occurs when trees
196 are allocated an inadequate space: as the tree grows up, the roots start spreading and
197 making their way underneath buildings (Day, 1991). The pressure that roots are capable
198 of exerting is fairly weak and is further diminished by urban soil compaction (Roberts, et
199 al., 2006). Moreover, modern building foundations are designed to withstand root-
200 induced movement.

201 Indirect damage is a more common cause of disturbance to structures, especially the
202 shrinkage of expansive soils (Driscoll, 1983). Roots belonging to trees growing close to
203 buildings tend to develop under the foundations, as the moisture content there tends
204 to be higher than in the surrounding soil (Figure 2). The extraction of water by roots
205 creates a reduction in soil volume, resulting in subsidence and cracks in the structures
206 (Day, 1991).



207

208

Figure 2: Tree roots growing under foundations

209 Cutler and Richardson (1981) and Biddle (2001) have reviewed several cases of damage
210 to buildings, producing an extensive analysis of how tree root interaction with the
211 surrounding environment can damage buildings. Regarding damage to ancient
212 structures, Caneva, Ceschin and De Marco (2006) have carried out a risk evaluation of
213 root-induced damage which archaeological sites are exposed to, while Caneva et al.
214 (2009) have surveyed the archaeological site of Villa Torlonia in Italy, investigating the
215 root expansion and evaluating the tendency of various species to harm ancient
216 monuments.

217 **3.2.2. Utilities**

218 Underground services, especially sewers, are frequently obstructed or damaged by the
219 growth of roots. This damage usually occurs in old systems (Randrup, et al., 2001), as
220 these were built with materials which could deteriorate with time, such as bricks or
221 concrete. Moreover, roots are attracted by the presence of moisture around pipes,
222 which are commonly cooler than the surrounding soil (Brennan, et al., 1997) and tend
223 to grow around the pipe (Figure 3).



224

225

Figure 3: Roots growing around a pipe

226

227 Modern sewers are made of plastic, iron or reinforced concrete, which are unlikely to
228 be damaged by root growth pressure. Potential leakages due, for example, to a broken
229 joint (Schrock, 1994) or poor construction (Sullivan, et al., 1977) (Brennan, et al., 1997)
230 can lead to roots penetrating the pipe, and eventually blocking it.

231 **3.2.3. Roads and pavements**

232 Urban trees provide several environmental, social and economic benefits, but they can
233 also cause extensive damage to road infrastructures. Root development can cause
234 disruptions to road surfaces, such as cracking or uplifting (Francis, et al., 1996) (Figure
235 4). This damage can have serious consequences (Tosti, et al., 2018a), leading to
236 additional pavement maintenance or repair and interventions on the tree (Mullaney, et
237 al., 2015).



238

239

Figure 4: Damages to road pavement due to tree roots

240 One of the principal causes of conflict between roots and infrastructures seems to be
241 the limited space provided for the development of trees (Barker, 1983) (Francis, et al.,
242 1996). Tree size at maturity should be considered when choosing tree species to plant,
243 as it will influence the necessary volume of soil (Trowbridge & Bassuk, 2004). Such
244 amounts of soil are not typical of urban environments, and trees are usually confined to

245 tree lawns, which restrict not only the roots but also the branch and canopy
246 development (Pokorny, et al., 2003). Also, trunk flare and root buttresses are associated
247 with road infrastructure damages (Wagar & Barker, 1983), and the tendency of species
248 to develop them should be considered when choosing which tree to plant (Costello &
249 Jones, 2003). Finally, when large trees are planted in cities, there is a significant danger
250 of wind-throw, as tree roots are often cut during pavement repairs and therefore cannot
251 offer sufficient resistance to wind load (Pokorny, et al., 2003). Therefore, a selection of
252 species adequately matched to the site conditions is advisable (Costello & Jones, 2003),
253 as this can lead to a significant reduction of hazards; however, McPherson and Peper
254 (2000) state that this resolution would reduce the benefits gained from larger trees.

255 Another factor which limits root development is soil compaction, as it decreases soil
256 aeration, restricts air and water movement, limits water-holding capacity and impedes
257 root penetration (Boyer, 1995). This is a significant issue in urban areas, as it conflicts
258 with road engineering specifications, which require a load-bearing base to support
259 pavement loading (Grabosky, et al., 1998). The essential requirement is to increase soil
260 compaction in order to reduce cavities and increase contact between the grains, thus
261 giving the lithic structure a high frictional resistance. Moreover, this minimises deferred
262 subsidence, providing greater functionality and security to the infrastructure. The
263 resulting level of compaction produces unbearable conditions for root growing (Blunt,
264 2008) (Grabosky, et al., 2009) as it limits access to oxygen, water and nutrients (Loh, et
265 al., 2003) (Lucke, et al., 2011) (Tracy, et al., 2011). Table 1 compares the prescriptions
266 for bulk densities of soils based on the Proctor Compaction Test (ASTM D698/AASHTO
267 T99) with the maximum level of compaction, which inhibits root penetration.

268

Bulk density of soils at 70 - 95% relative compaction						
		Landscape		Paving		Critical bulk density
		70%	85%	90%	95%	
Soil type	Loamy sand (WG)	1.52	1.85	1.96	2.07	1.75
	Sandy loam (WG)	1.43	1.74	1.85	1.95	1.70
	Sandy loam (MG)	1.35	1.64	1.74	1.83	1.70
	Sandy silty clay	1.29	1.56	1.66	1.75	1.50
	Silt	1.19	1.45	1.53	1.62	1.40
	Silty clay	1.22	1.49	1.58	1.66	1.40
	Clay	1.15	1.40	1.49	1.57	1.40

269 Table 1: Information on the critical bulk density for soils of differing textures (ASTM D698/AASHTO T99). Critical
270 bulk density is the level of compaction at which the roots are no longer able to penetrate the soil. Units are given
271 as dry bulk density in grams per cubic centimetre (gm/cc). WG is with gravel; MG is minus gravel (Lindsey & Barlow,
272 1994)

273 Such levels of compaction cause roots to develop at the interface between the
274 pavement and soil, where nutrients and moisture are available (Kopinga, 1994)
275 (Randrup, et al., 2001) (Wagar & Franklin, 1994). The favourable conditions that roots
276 find at the interface between the surface layer and the sub-base make them grow faster,
277 resulting in accelerated secondary thickening that can cause damage to the road surface
278 (Nicoll & Armstrong, 1998).

279 Other issues that can interfere with root growth in urban environments and lead to road
280 infrastructure damage are waterlogging (Boyer, 1995) (Pokorny, et al., 2003) and severe
281 water deficiency (Boyer, 1995) (Mullaney, et al., 2015). In the former case, soil
282 saturation displaces air, making soil aeration more restrictive as depth increases and
283 therefore forcing roots to grow within the soil surface; these conditions encourage the
284 development of root pathogens. In the latter case, water deficit causes trees to slow
285 down their leaf growth, resulting in a surplus of carbohydrates, which then become
286 available for root growth. The immediate consequence, therefore, is that the root
287 dimensions of water-stressed plants are higher than average.

288

289 **4. Detection and Mapping of Tree Root Systems**

290 Locating tree roots and estimating their depth and spread is a significant challenge, and
291 a necessary condition for several practices, ranging from tree health preservation to
292 safety assessment in urban areas. There are several methods for studying roots
293 available, which can be divided into destructive or non-destructive techniques.

294 **4.1. Destructive testing methods**

295 Destructive testing methods allow for the investigation of root systems at the time of
296 sampling. Therefore, they are of limited value for investigating developmental
297 processes. Moreover, these techniques are not only destructive to the root system itself
298 and its immediate environment (Taylor, et al., 1991), but are also expensive, time-
299 consuming and laborious (Krinskyukov & Lyaksa, 2016). Given root system architecture
300 variability, several replicated samples are needed to precisely assess root parameters,
301 but this practice destroys the roots and exposes the tree to diseases and infections that
302 can lead to its death (Smit, et al., 2013). However, these techniques are still widely used,
303 as they provide reliable quantitative results.

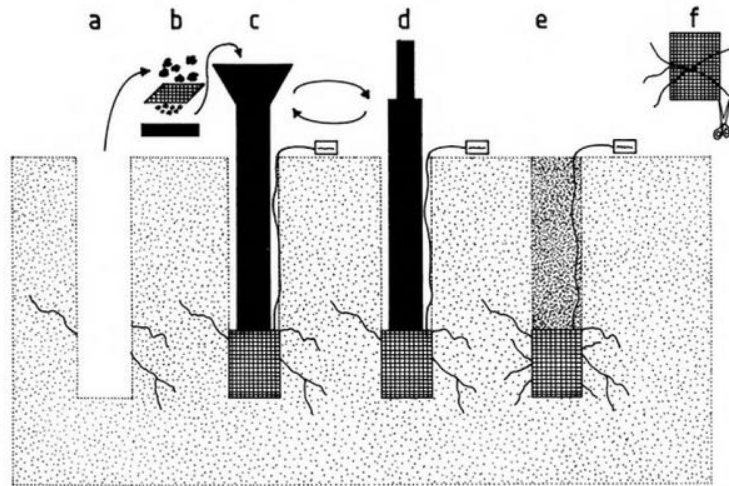
304 The main destructive techniques are:

- 305 • Ingrowth core;
- 306 • Auger method;
- 307 • Monolith method.

308 **4.1.1. Ingrowth core**

309 Ingrowth cores are commonly used to quantify fine root production and to estimate the
310 rate of growth during a given period (Smit, et al., 2013). They are also adopted to
311 examine the effect of experimental manipulation on root growth (Majdi, et al., 2005).
312 The operating principle of this technique is to replace a volume of soil (as it is) with the
313 same volume of root-free soil, enclosed in a mesh bag, which is resampled after a
314 determined period (Figure 5). This method is widely acknowledged to be straightforward
315 and inexpensive, and it illustrates how long it takes for roots to develop in a particular
316 soil. However, it can lead to misinterpretation, as the soil structure is altered when the

317 mesh bags are introduced into the cores (Smit, et al., 2013) and this can affect root
318 growth rates. Moreover, since roots are damaged by the initial coring, their
319 development into the root-free samples can be unnatural (Majdi, et al., 2005).



320

321 **Figure 5: Procedure for installing the mesh bags for the root ingrowth core technique (Smit, et al., 2013).** a) a core
322 of soil is removed and b) the soil is sieved to remove the roots; c) a mesh bag is placed in the hole, which is filled
323 with the sieved soil; d) the soil is packed to the original bulk density by means of a pestle; e) the mesh bag is left
324 in place for a determined period of time, after which it is recovered and f) non-woody roots are trimmed.

325 **4.1.2. Auger method**

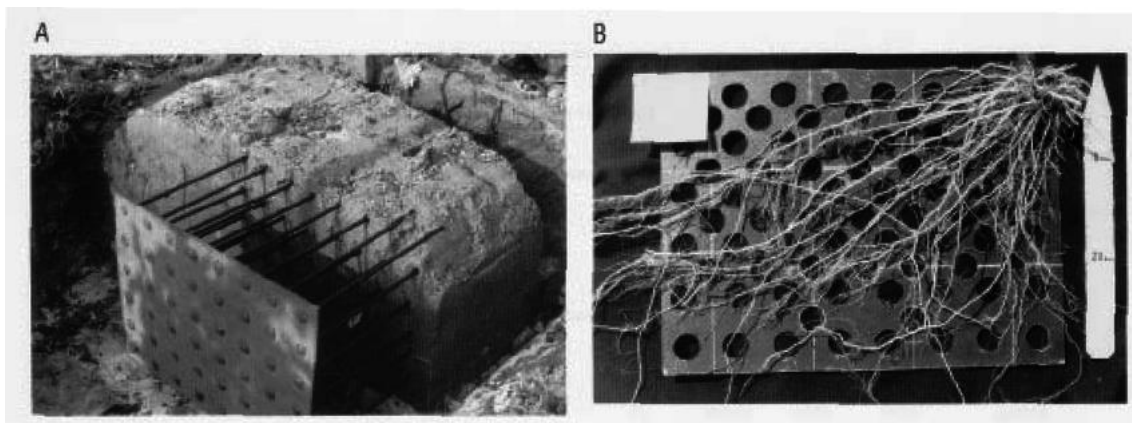
326 The auger method is the most convenient for investigating root density. It involves
327 taking soil samples from the field, which are then washed to separate roots from the soil
328 (Bohm, 2012) (Smit, et al., 2013). The soil core extraction can be made using either a
329 hand-operated or a mechanical sampler, depending on the hardness of the investigated
330 soil. The former is faster to use, being a cylindrical tube 15 cm long with an inside
331 diameter of 7 cm, equipped with a T-handle at the top that simplifies the penetration
332 into the soil by rotation. However, if core samples need to be taken from hard soil or
333 considerable depths, the auger is driven into the soil by a motorised dropping hammer,
334 and then pulled back using a screw-jack (Smit, et al., 2013).

335 There exists uncertainty about the frequency of samples required in order to obtain
336 reliable results (Bohm, 2012), however, increasing the number of samples will lower the
337 uncertainty and improve the variability of data collected (Smit, et al., 2013).
338 Consequently, this technique is time-consuming (Majdi, 1996) and the large number of

339 replicates required harms a considerable part of the investigated root system (Smit, et
340 al., 2013). Moreover, the type of soil can prevent the sampler from being inserted, such
341 as in stony or dry clay soils (Smit, et al., 2013).

342 **4.1.3. Monolith method**

343 The monolith method requires large blocks of soil to be removed and washed out, in
344 order to separate the roots from the soil (Boyer, 1995) (Bohm, 2012). Contrary to the
345 auger method, which requires just the root volume to be quantified, in this technique
346 roots are washed without displacing them from their original position (Weaver & Voigt,
347 1950). This is possible thanks to the use of special boards covered with spikes, called
348 pinboards, which are driven into the soil to preserve the root architecture while the soil
349 is washed away (Boyer, 1995) (Figure 6).



350

351 **Figure 6: Metallic monolith pinboard used for excavating the soil-root samples (left) and roots after extraction**
352 **and washing from the soil (right) (Leskovar, et al., 1994)**

353 This technique provides useful information, as it is possible to have a general view of the
354 root system architecture (Smit, et al., 2013). On the other hand, the collection of the
355 samples requires great skill in order not to displace the roots, so the pinboards are
356 usually of limited dimensions; additionally, the washing process can introduce biases, as
357 significant losses of fine roots can occur (Smit, et al., 2013). Finally, this method is often
358 non-repeatable, as the hole will be filled up with new soil that could lead the roots to
359 develop differently, affecting the results of a second inspection (Schuurman &
360 Goedewaagen, 1965).

361

362 **4.2. Non-destructive testing methods**

363 Non-destructive evaluations are acknowledged as being effective in investigating
364 different materials, without harming or damaging them (Buza & Divos, 2016).
365 Furthermore, these techniques are easily repeatable, which means that long-term
366 investigation and monitoring of trees can be achieved (Buza & Divos, 2016).

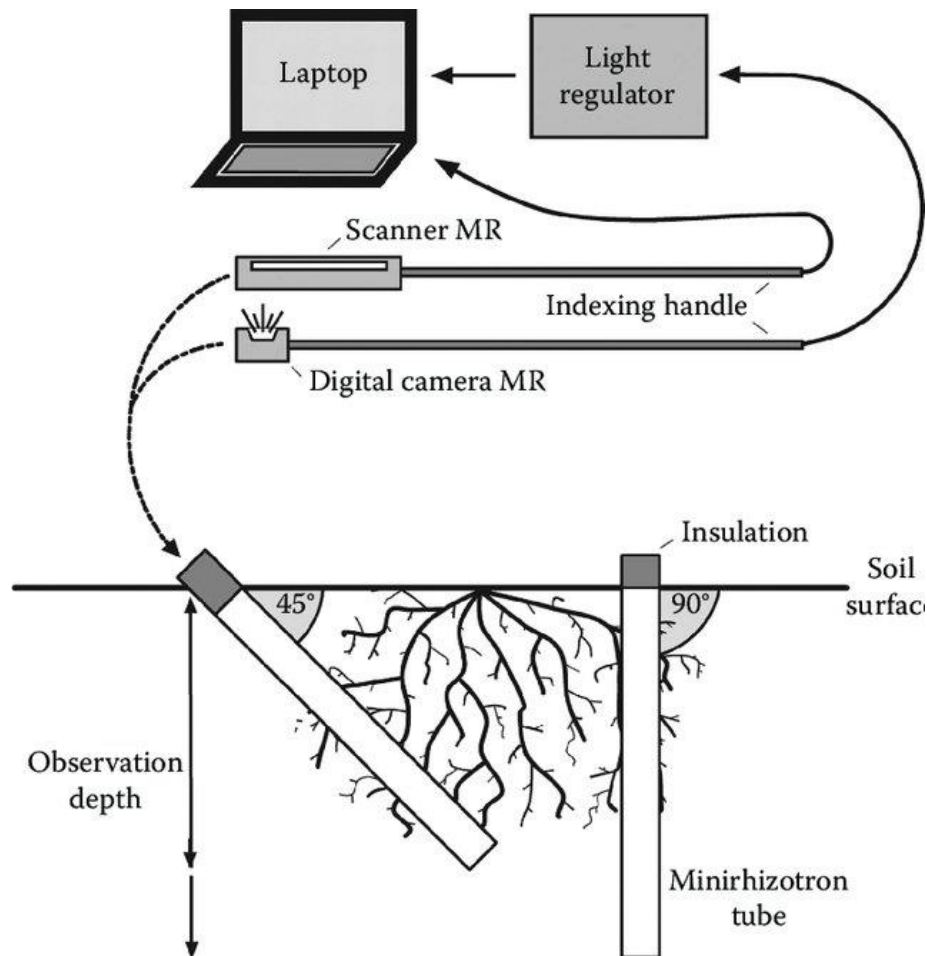
367 The main non-destructive techniques applied in root system investigations are:

- 368 • Rhizotrons and minirhizotrons;
- 369 • Pulling test;
- 370 • Electrical resistivity tomography (ERT);
- 371 • Acoustic detection;
- 372 • X-ray computed tomography (CP);
- 373 • Ground penetrating radar (GPR).

374 **4.2.1. Rhizotrons and minirhizotrons**

375 One of the first NDT methods for tree root system observations was to put glass plates
376 into the soil, so that it was possible to observe root development and growth against
377 them. This method has evolved into the modern rhizotron, namely an underground
378 chamber equipped with glass walls (Boyer, 1995).

379 This technique provides repeated and non-destructive access to soil and roots, allowing
380 for a better understanding of underground processes as they are in nature.
381 Nevertheless, since such an instalment is impossible to set up for assessment of urban
382 trees, minirhizotrons have become increasingly popular. These instruments consist of
383 small plastic tubes (about 5 cm in diameter and 2 to 3 m long), which can be driven into
384 the ground at different angles (Majdi, 1996). A fibre optic light and a camera are then
385 lowered down the tube, in order to observe the roots' developmental process over time
386 (Boyer, 1995), sometimes in combination with dedicated image processing software
387 (Majdi, 1996) (Figure 7).



388

389 **Figure 7: Minirhizotron typical setups (diagonal and vertical installation) (Eshel & Beeckman, 2013)**

390 This method is commonly used for quantitative investigations on root length production,
 391 root length mortality, longevity, rooting density and root diameter, as well as to achieve
 392 qualitative information about root colour, branching and decomposition (Majdi, 1996).

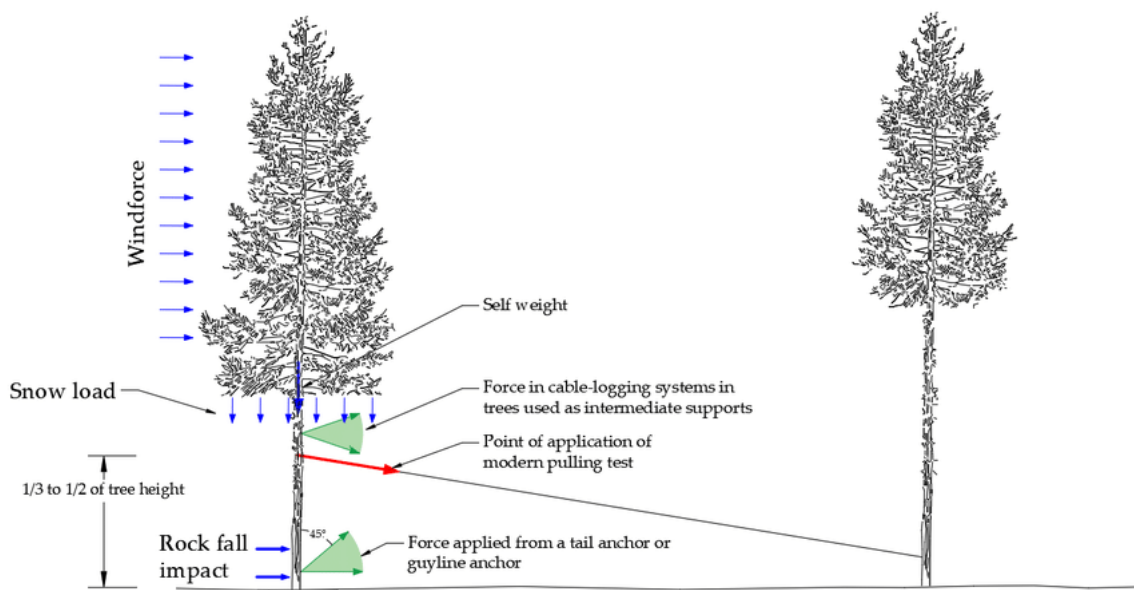
393 The main limitations of this technique are linked to its installation in hard or stony soils
 394 (Majdi, 1996). Moreover, the viewing window is static, providing only a limited, 2-D
 395 visualisation that is unrepresentative of the architecture of a tree root system (Mooney,
 396 et al., 2012). Another limitation arises from the fact that rhizotrons are not totally non-
 397 invasive, as they may create an altered soil-root interface that could affect root growth
 398 (Amato, et al., 2009) (Neumann, et al., 2009). Finally, the effectiveness of minirhizotrons
 399 as opposed to other techniques, especially when used in the shallow subsurface, is still
 400 an object of discussion (Heeraman & Juma, 1993).

401

402 **4.2.2. Pulling test**

403 The pulling test is principally applied to test the root system anchorage to the soil. Its
404 primary application is the assessment of the reaction of the tree to a determined load,
405 especially the one caused by the wind (Buza & Divos, 2016), in terms of the resulting
406 bending of the stem and the inclination of the root plate (Fay, 2014).

407 During a pulling test, a load is applied to the subject tree by securing a cable to the tree
408 trunk. The pulling force applied using a load cell or force meter is measured, and factors
409 such as the inclination, elongation and dislocation of the ground are monitored (Buza &
410 Divos, 2016) (Marchi, et al., 2018). In order to evaluate the risk of tree uprooting, an
411 inclinometer is applied to the trunk close to the ground. Depending on the tree species
412 and conditions, limits are placed on the possible inclination of the tree, in order to
413 prevent damage to tree roots. Destructive pulling tests were conducted in several
414 studies (Coutts, 1983) (Brudi & Wassenaer, 2002) (Lundström, et al., 2007), which report
415 root failure models and maximum inclination values for different tree species.



417 **Figure 8: Schematic representation of a pulling test (Marchi, et al., 2018)**

418 The primary output of a pulling test is a safety factor, which is given by the ratio between
419 the tree capacity and the calculated load (Buza & Divos, 2016). According to field studies
420 (Fay, 2014), a tree is considered stable when its safety factor is greater than 1.5.

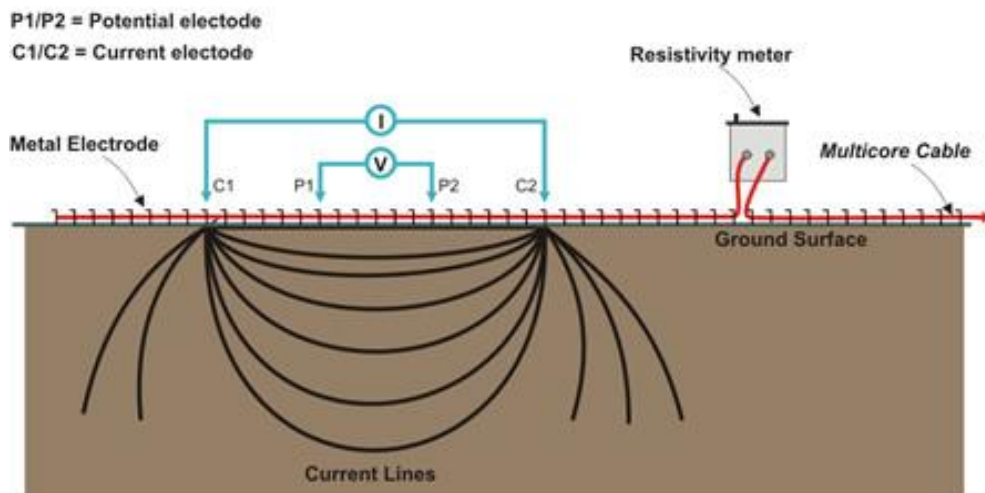
421 The pulling test provides useful information on the stability of trees, evaluating their
422 resistance to external loads. It can be performed not only to assess the tree root plate
423 conditions, but also the status of the trunk in terms of maximum bending moment (Fay,
424 2014). However, the main limitation of this method is that it is not completely non-
425 invasive, as both the trunk and the roots can be damaged when the pulling force is
426 applied (Marchi, et al., 2018).

427 Other limitations to this methodology arise from the fact that the applied load cannot
428 represent the complex action of the wind, but can only cause a reaction in the tree which
429 can be compared to the one produced by the wind load (Fay, 2014). Moreover, the test
430 could be affected by factors such as the temperature conditions of both the soil and the
431 tree (Buza & Divos, 2016). Finally, the pulling test cannot predict the moment or the
432 conditions under which the tree will fail (Fay, 2014), but can only assess the conditions
433 of the tree at the time of testing.

434 **4.2.3. Electrical resistivity tomography**

435 Electrical resistivity tomography (ERT) is a geophysical technique used for the calculation
436 of the subsurface distribution of soil electrical resistivity (Zenone, et al., 2008). Electrical
437 resistivity (ρ) is defined as the electrical resistance through a uniform body of unit length
438 and unit cross-sectional area and represents a measure of the ability of materials to limit
439 the transfer of electrical current. This method has been extensively used for the
440 characterisation of soil heterogeneity.

441 Soil resistivity is measured by applying electric currents through at least two conductors
442 (current electrodes) and measuring the resulting differences in electric potential
443 (voltage) on at least two separate conductors (potential electrodes). There are different
444 possible geometric configurations for electrodes. The potential electrodes could be
445 placed between the current electrodes (Wenner array, Figure 9) or consecutive to them
446 (dipole-dipole configuration). The investigation depth relies on the configuration choice,
447 and increases with the spacing between electrodes (Amato, et al., 2009).



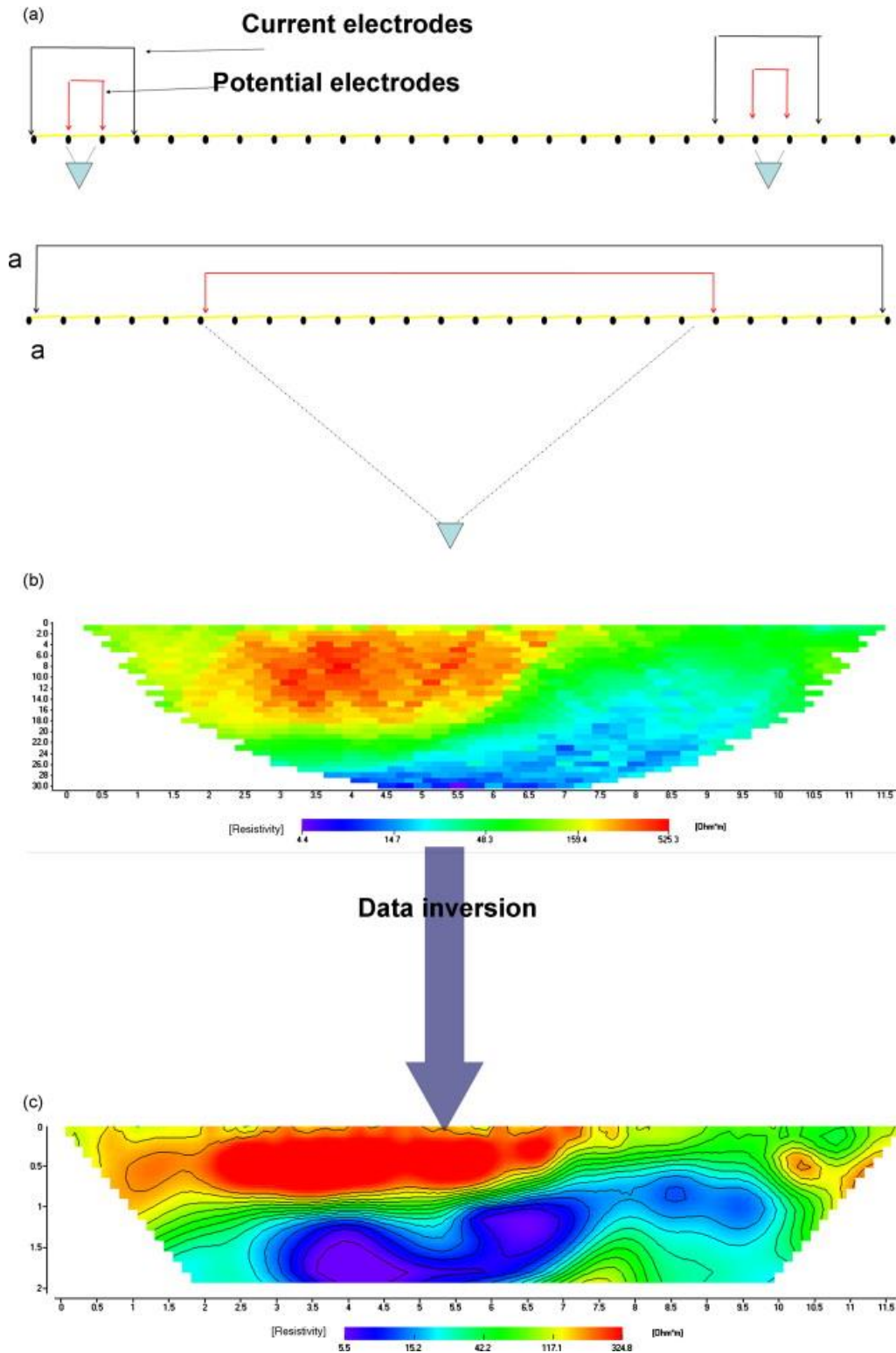
448

449

Figure 9: General ERT operating principles for a Wenner array configuration

450 The voltage distribution in space is a function of the different resistivity of soil volumes
 451 (Kearey, et al., 2013).

452 Geophysical surveys performed using electrical exploration have qualitative purposes,
 453 and are based on the contrast between the resistivity of different soil layers or the
 454 heterogeneous materials within each layer. In heterogeneous media, the current flow
 455 lines are deformed and tend to be concentrated in conductive volumes. Resistivities are
 456 first calculated according to the theoretical flow-line distribution in isotropic media and
 457 are called apparent resistivity values. These are attributed to soil coordinates
 458 corresponding to the hypothesis of homogeneous current distribution and arranged in
 459 a pseudosection. In order to obtain real resistivity values, correctly positioned in space
 460 (true section), a procedure called inversion is applied. The investigated soil domain is
 461 divided into elementary cells, and resistivity data are imaged by attributing values
 462 corresponding to each elementary soil volume to a point corresponding to the
 463 intersection of two lines conducted through the centres of the quadrupoles (Figure 10)
 464 (Amato, et al., 2009).



465

466 Figure 10: Data acquisition and processing in ERT; (a) a linear array of electrodes with two quadrupoles at minimum
 467 spacing (top) and one quadrupole at maximum spacing (bottom). Dots represent electrodes and full triangles
 468 represent the centre of soil volumes measured by the corresponding quadrupole; (b) soil apparent resistivity 2D
 469 pseudosection obtained after data acquisition; (c) soil resistivity 2D section obtained after data inversion with
 470 numerical modelling (Amato, et al., 2009)

471 ERT has been widely applied for detecting soil compaction (Besson, et al., 2004), water
472 content and flow in soil and plants (Loperte, et al., 2006), soil cracks (Samouelian, et al.,
473 2005) and tillage effects (Basso, et al., 2010). The plant root zone shows variations in soil
474 electrical resistivity (Panissod, et al., 2001), and resistive soil volumes have been
475 correlated to large tree root structures (Amato, et al., 2008) (Zenone, et al., 2008).

476 Amato, et al (2008) conducted research in which the root biomass of alder trees was
477 accurately mapped in 2D. This study demonstrated that the use of ERT for the non-
478 destructive characterisation of root systems' spatial structure could reduce the
479 coefficient of variability of root measurements, which is more significant than that of
480 above-ground plant parts (Amato & Ritchie, 2002).

481 A quantitative relationship between the electrical resistivity of the soil and the biomass
482 of the roots has been widely demonstrated (Loperte, et al., 2006) (Amato, et al., 2008).
483 However, in the case of low root biomass densities, the electrical response of the roots
484 is indistinguishable from the background noise. In fact, it is assumed that it is of the same
485 order of magnitude as the response coming from the other characteristics of the soil,
486 and consequently too weak to be detected (Amato, et al., 2009).

487 The main advantage of this technique is that it is totally non-destructive, as it does not
488 disturb the structure nor the functioning of soil. Subsurface heterogeneities can be
489 determined, in one, two or three dimensions, both non-invasively and dynamically
490 (Samouelian, et al., 2005). Variations in time of root systems can be obtained, and
491 different and more detailed information can be obtained by varying the operating
492 configurations or the distance between the electrodes, depending on soil properties.
493 Furthermore, this methodology has a low application cost, and can be applied on a large
494 scale.

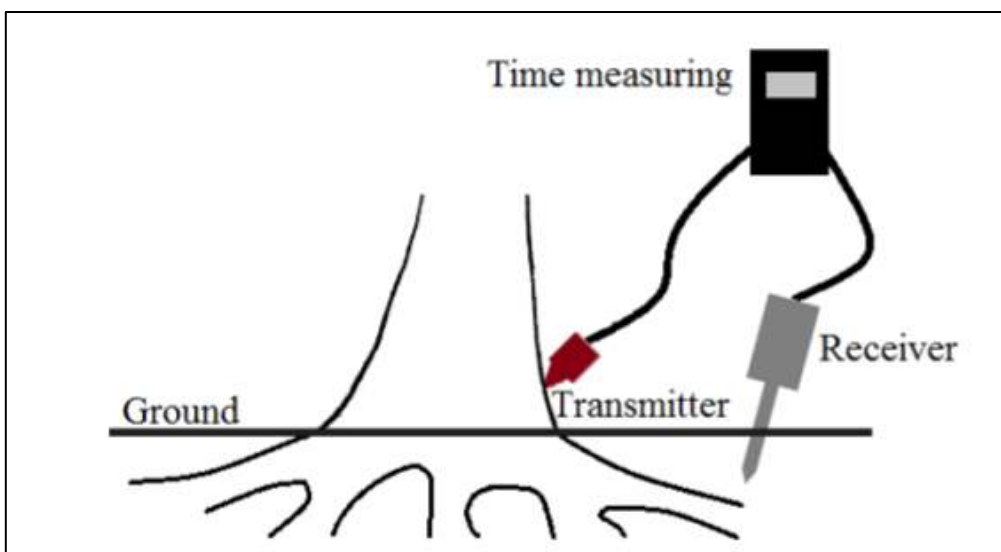
495 However, this investigation technique can be influenced by several factors, which could
496 potentially act at the same time, making interpretation of the results difficult.
497 Systematic errors can result from poor electrode contact or noise averaging, although
498 these can be avoided by carrying out replicated and reciprocal measurements (positive
499 and negative current and potential electrodes reversed) (Samouelian, et al., 2005).

500 Moreover, ERT field investigations should be coupled with laboratory studies, to
501 calibrate the resistivity against different soil conditions. (Samouelian, et al., 2005).

502 **4.2.4. Acoustic detection**

503 The acoustic detection of wood is widely used for tree investigations, ranging from the
504 detection of decay, cracks, hollows or holes (Buza & Goncz, 2015) (Wang, et al., 2007)
505 (Grabianowski, et al., 2006) to material characterisation for wood evaluation and quality
506 assessment (Bucur, 2006). Therefore, the acoustic detection of roots has been tested,
507 based on the difference of velocity in wood and soil. In fact, the velocity of the acoustic
508 signal in soil is between 250 – 400 m/s, depending on soil type and moisture content,
509 while the velocity in wood is between 2000 and 4000 m/s (Bucur, 2006) (Buza & Goncz,
510 2015).

511 The device for acoustic measurements consists of a transmitter, a receiver, and a time-
512 measuring component. The transmitter is needle-like and must be placed onto the trunk
513 at ground level, while the receiver is a long metal spike (30 cm or longer), which has a
514 suitable coupling for the soil (Figure 11) (Buza & Goncz, 2015). During an investigation,
515 the transmitter sends a very short signal, which is then reflected and read by the
516 receiver. The presence of roots decreases the travel time significantly, making it possible
517 to locate them.



518

519

Figure 11: Device for acoustic detection of roots (Buza & Goncz, 2015)

520 Using this technique, it is possible to identify roots with a diameter of 4 cm upwards,
521 with a maximum depth of investigation of 50 cm. Furthermore, it is possible to separate
522 two roots from each other if they are at least 20 cm apart (Buza & Divos, 2016). These
523 achievements are limitations as well, as the detection of small or deep roots is not
524 possible. Furthermore, research carried out by Iwase, et al. (2015) demonstrated that
525 the signal is highly sensitive to water content. Finally, other buried objects, such as rocks,
526 can disguise the signal, making it difficult to recognise root system architecture correctly
527 (Divos, et al., 2009). Given that this methodology, despite the promising results, is still
528 in its infancy, it is often coupled with other NDT methods, in order to further investigate
529 its potential (Buza & Goncz, 2015).

530 **4.2.5. X-ray computed tomography**

531 X-ray computed tomography (CT) is a non-destructive, non-invasive technique that can
532 be used to visualise the interior of objects in 2D and 3D based on the principle of
533 attenuation of an electromagnetic wave. X-ray CT has been repeatedly demonstrated to
534 be an efficient methodology for imaging and studying soil systems. CT uses X-rays to
535 obtain cross-sectional images of an object, which contain information regarding the
536 attenuation of the X-rays, a function of the density of the sample material (Mahesh,
537 2002). These slices are then reconstructed to provide a 3-D visualisation of the sample
538 volume.

539 During CT acquisition, X-rays are produced in a highly evacuated tube, which contains
540 an anode, usually platinum or tungsten, and a cathode (Wildenschild, et al., 2002). When
541 a high voltage is applied across these electrodes, accelerated electrons produce X-rays
542 as they strike the anode. As the X-ray beams pass through a sample, the object itself
543 becomes a secondary source of X-rays and electrons. A portion of the primary incident
544 beam is therefore absorbed or scattered. This reduction in intensity of the X-ray as it
545 passes through the investigated object is called attenuation. The beam is projected onto
546 the detector, which measures the change in energy intensity (Mooney, et al., 2012).

547 X-ray CT offers great potential for examining undisturbed root systems architecture in
548 soils, and its potential has been widely investigated within the last decades (Heeraman,

549 et al., 1997) (Gregory, et al., 2003). The imaging of plant roots in soil using X-ray CT relies
550 on sufficient contrast in X-ray attenuation between growth medium solids, air-filled
551 pores, soil water, plant material and organic matter. The attenuation of these materials
552 varies with several factors including soil type, soil moisture content, the proximity of
553 roots to organic matter or air-filled pores and root water status (Kaestner, et al., 2006).

554 The limitations of this technique are the overestimation of root diameter during image
555 analysis due to the proximity of water and air within the soil (Perret, et al., 2007), and
556 the underestimation of root length and number of lateral roots due to the fact that root
557 material cannot be easily distinguished from other soil components. To minimise the
558 effects of similar attenuation between the soil and plant fractions, researchers have
559 focused on plants with coarse roots (Hargreaves, et al., 2009), artificial soil systems
560 (Perret, et al., 2007), manipulating the water content of the sample and undertaken
561 convoluted image processing to enhance contrast. Still, it is difficult to distinguish the
562 boundaries between adjacent structures (Mooney, et al., 2012).

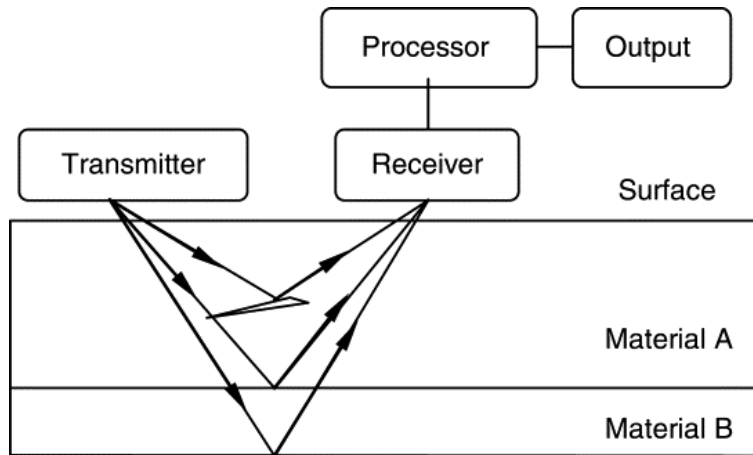
563 Advancements in CT technology include a reduction in scan and reconstruction times by
564 at least an order of magnitude, automated algorithms to remove artefacts and more
565 sophisticated detectors that have significantly increased the raw scan image quality
566 (Mooney, et al., 2012). Research is now focused on investigating this technique's future
567 potential in terms of the interaction between roots and their soil environment (Tracy, et
568 al., 2010).

569 **5. Ground Penetrating Radar**

570 Ground penetrating radar (GPR) is a non-destructive testing method used to detect
571 changes in physical properties within the shallow subsurface (Daniels, 1996). The
572 operating principles of a GPR system are based on the theory of electromagnetic (EM)
573 fields, which is described by Maxwell's equations (Jol, 2008). In addition, GPR
574 effectiveness relies on the response of the investigated materials to the EM fields, which
575 is ruled by the constitutive equations (Jol, 2008). Therefore, the combination of the EM
576 theory with the physical properties of the material is essential for a quantitative
577 description of the GPR signal.

578 **5.1. GPR theoretical background**

579 A standard GPR system consists of three essential components: a control unit (including
580 a pulse generator, computer, and associated software), antennas (including paired
581 transmitting and receiving antennas), and a display unit (Guo, et al., 2013) (Figure 12).
582 During a GPR investigation, the transmitting antenna generates short impulses of EM
583 energy, which are launched into the investigated medium where they propagate as
584 waves (Daniels, 1996). When these waves hit a target with different electrical or
585 magnetic properties, reflections are generated, which are then diffracted back towards
586 the surface and recorded by the receiving antenna. The remaining energy, conversely,
587 continues to travel into the medium until it is completely attenuated (Daniels, 1996).
588 The control unit samples and filters the collected information, and then combines it into
589 a reflection trace (also named A-scan), recording the time between the emission of the
590 reflected signal and its reflection on the vertical axis and the amplitudes of the received
591 signals on the horizontal axis (Daniels, 2004). Being an individual trace, the A-scan
592 provides punctual information about the subsurface configuration (Benedetto, et al.,
593 2017).



594

595

Figure 12: GPR operating principles

596 The depth of a target can be derived from the propagation velocity (V), as follows
 597 (Daniels, 1996):

$$D = \frac{V \times t}{2} \quad (1)$$

598 where D is the depth and t is the two-way travel time. Instead, wave velocity can be
 599 calculated from the following equation (Lorenzo, et al., 2010):

$$V = \frac{1}{\sqrt{\frac{\mu\varepsilon}{2} \left(\sqrt{1 + \left(\frac{\sigma}{\omega\varepsilon} \right)^2} \right) + 1}} \quad (2)$$

600 where

- 601 • μ is the magnetic permeability;
- 602 • σ is the electrical conductivity;
- 603 • ε is the dielectric permittivity;
- 604 • ω is the angular frequency ($\omega = 2\pi f$, where f is frequency) of the emitted
 605 pulse.

606 A formula for the estimation of propagation velocity for low conductive and
 607 nonmagnetic materials ($\sigma \ll \omega\varepsilon$ and $\mu_r = 1$, where μ_r is the relative magnetic
 608 permeability) has also been proposed (Jol, 2008) (Daniels, 2004):

$$V = \frac{1}{\sqrt{\mu\varepsilon}} = \frac{c}{\sqrt{\varepsilon_r}} \quad (3)$$

609 where

- 610 • c is the speed of light in vacuum (0.2998 m per nanosecond);
- 611 • ε_r is the relative dielectric permittivity.

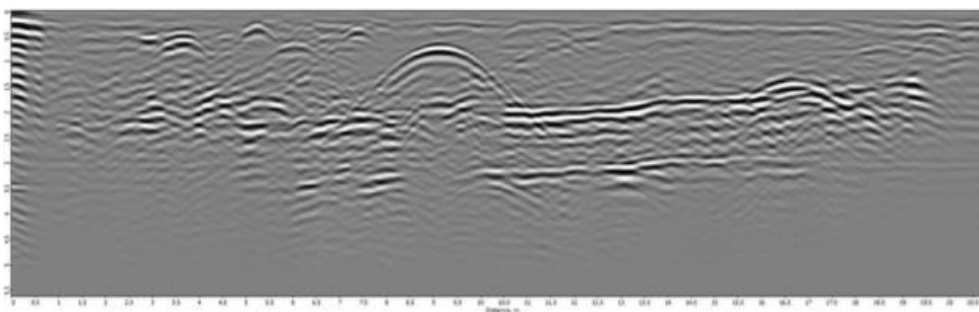
612 The reflected energy amplitude at an interface between two materials depends on the
 613 reflection coefficient R (al Hagrey, 2007):

$$R = \frac{\sqrt{\varepsilon_{r1}} - \sqrt{\varepsilon_{r2}}}{\sqrt{\varepsilon_{r1}} + \sqrt{\varepsilon_{r2}}} = \frac{V_2 - V_1}{V_1 + V_2} \quad (4)$$

614 where

- 615 • ε_{r1} is the relative dielectric permittivity of the overlying material;
- 616 • ε_{r2} is the relative dielectric permittivity of the underlying material;
- 617 • V_1 is the propagation velocity in the overlying material;
- 618 • V_2 is the propagation velocity in the underlying material.

619 During a survey, GPR is moved along a detection transect, and EM pulses are generated
 620 at a specified interval of time or distance. As reflected signals are recorded, traces can
 621 be integrated into a radargram (also called B-scan) that allow for a 2D representation of
 622 the subsurface (Figure 13). The B-scan mode is a widely used imaging methodology, as
 623 it permits to visualise the presence of buried objects (Bianchini Ciampoli, et al., 2019).



624

625

Figure 13: A typical radargram or Bscan

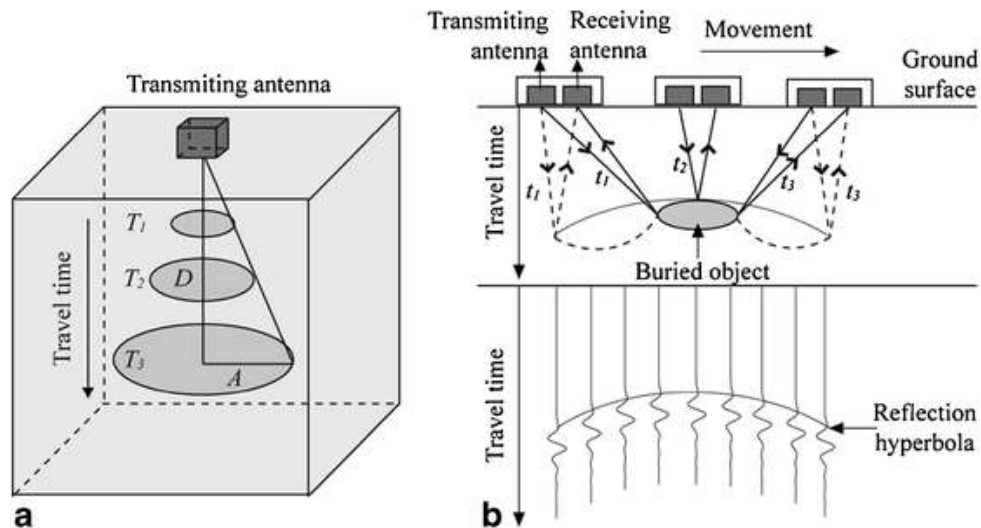
626 The GPR transmitting antenna produces energy in the form of a beam that penetrates
627 into the ground in the form of an elliptical cone. As the propagation depth increases, the
628 cone radius also expands, resulting in a larger footprint scanned beneath the antenna
629 (Figure 14a). The footprint area can be approximated by the formula (Conyers, 2002):

$$A = \frac{\lambda}{4} + \frac{D}{\sqrt{\epsilon_r + 1}} \quad (5)$$

630 where

- 631 • A is the long dimension radius of footprint;
- 632 • λ is the centre frequency wavelength of radar energy;
- 633 • D is the depth from the ground surface to the reflection surface;
- 634 • ϵ_r is the average relative dielectric permittivity of scanned material from the
635 ground surface to the depth of reflector (D).

636 Based on this feature of propagating waves, radar energy will therefore be reflected
637 before and after the antenna is positioned above a buried object. As the antenna moves
638 closer to the object, the recorded two-way travel time decreases, while when the
639 antenna moves away from it, the same phenomenon is repeated conversely, generating
640 a reflection hyperbola, the apex of which indicates the exact location of the buried
641 object (Guo, et al., 2013) (Figure 14b).



642

643 **Figure 14: Schematic illustration of the conical radiating pattern of GPR waves and generation of a reflection**
 644 **hyperbola (Guo, et al., 2013): a) development of a footprint with increasing travelling time; b) detection of a**
 645 **buried object with the creation of a reflection hyperbola**

646 The GPR resolution, and therefore its capability to discriminate between two closely
 647 spaced targets as well as the minimum size detectable, correlates negatively with the
 648 footprint area. GPR detection resolution depends on the antenna frequency, the EM
 649 properties of the medium, and the penetrating depth (Hruska, et al., 1999). Therefore
 650 in a survey, the selection of the appropriate GPR features, including frequency
 651 operations, the type of antenna or its polarization rely on a number of factors, such as
 652 the size and shape of the target and the transmission properties of the investigated
 653 medium, as well as the characteristics of the surface (Daniels, 2004).

654 Advances in GPR data processing and visualisation software have allowed for the
 655 creation of 3D pseudo-images (also called C-scans) of the subsurface, obtained by
 656 interpolating multiple 2D radargrams. A C-scan provides an amplitude map at a specific
 657 time (or depth) of collection (Benedetto, et al., 2017), and is therefore helpful in
 658 visualising a trend of the amplitude values all over the investigated domain.

659 In regard to GPR data processing and analysis, appropriate signal processing techniques
 660 are needed to provide easily interpretable images to operators and decision-makers
 661 (Daniels, 2004). Most of the techniques that are applied today originate from seismic
 662 theory (Benedetto, et al., 2017), as both disciplines involve the collection of pulsed
 663 signals in the time domain. It is not possible to establish a unique methodology, as it

664 depends on the purpose of the survey, the features of the used radar and the conditions
665 of the investigated medium. Furthermore, the analysis of GPR data is a challenging issue,
666 as the interpretation of GPR data is generally non-intuitive and considerable expertise is
667 therefore needed.

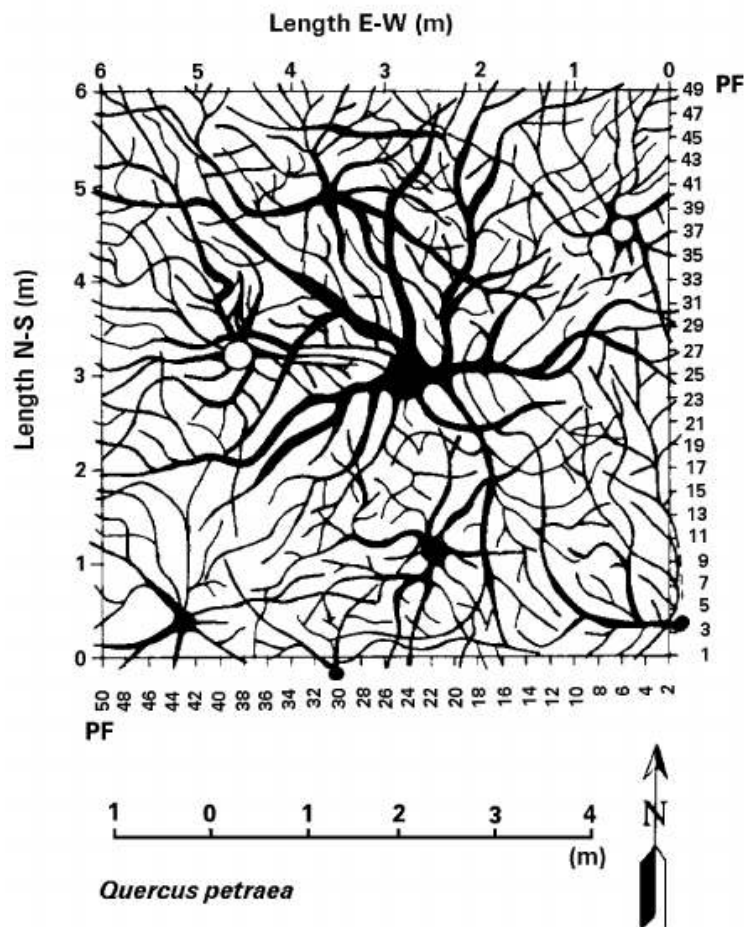
668 **5.2. GPR applications in the assessment of tree root systems**

669 GPR has been employed for many applications and in several disciplines, such as
670 archaeological investigations (Goodman, 1994), bridge deck (Alani, et al., 2013) and
671 tunnel analyses (Alani & Tosti, 2018), the detection of landmines (Potin, et al., 2006),
672 civil and environmental engineering applications (Tosti et al., 2018b) (Benedetto, et al.,
673 2017) (Benedetto, et al., 2015) (Loizos & Plati, 2007), and planetary explorations (Tosti
674 & Pajewski, 2015), for about forty years.

675 Although GPR has commonly been used to characterise soil profiles (Lambot, et al.,
676 2002) (Huisman, et al., 2003), roots have often been considered an unwanted source of
677 noise that usually complicates radar interpretation (Zenone, et al., 2008). However, over
678 the past decade, GPR has been increasingly used for tree root assessment and mapping,
679 as it is completely non-invasive and does not disturb the soils or bring harm to the
680 examined trees or the surrounding environment. For these reasons, repeated
681 measurements of root systems are possible, allowing for the study of the roots'
682 developmental processes.

683 The first application of GPR that relates to the mapping of tree root systems dates back
684 to 1999 (Hruska, et al., 1999). In this study, a GPR system with a central frequency of
685 450 MHz was employed to map the coarse roots of 50-year-old oak trees, and
686 measurements were made in two directions within a 6 m by 6 m square, with a 0.25 m
687 x 0.25 m profile grid, at 0.05 m intervals. After data processing, the root system of the
688 large oak tree was analysed in detail by applying depth correlations of GPR indications
689 from single profiles to develop a 3D picture. Additionally, the root system was excavated
690 and photographed, and root lengths and diameters were measured to verify the radar
691 data. The researchers confirmed that the resolution of the GPR system was sufficient to
692 distinguish the roots that were 3 cm to 4 cm in diameter. Diameters of roots detected

693 by the GPR system corresponded to measured diameters of excavated roots with an
 694 error of between 1 and 2 cm. The GPR system determined the length of individual roots,
 695 from the stem to the smallest detectable width, with an error margin of about 0.2 dm
 696 to 0.3 dm. Higher frequencies together with smaller measurement intervals were
 697 applied, and this method improved the resolution and accuracy to less than 1 cm. In
 698 conclusion, the researchers claimed to have successfully tested GPR in a forest and
 699 woodland environment, where the soil is relatively homogenous. The output of this
 700 study was criticised several years later (Guo, et al., 2013), because the 3D views of the
 701 coarse root system were redrawn manually based on the GPR radargram, but no specific
 702 information was provided regarding how it had been done (Figure 15). Assuming that
 703 the maps were redrawn arbitrarily according to the operator's personal experience, bias
 704 may therefore have been introduced.



705

706
 707

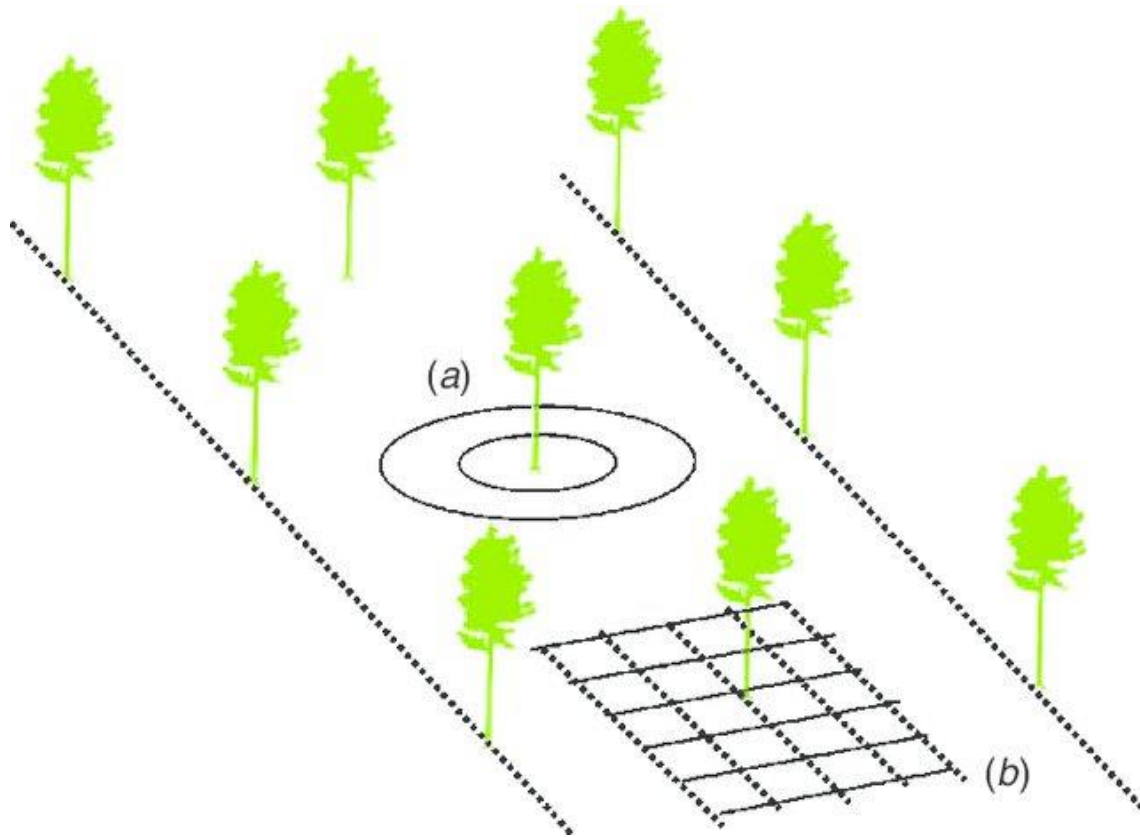
Figure 15: Hand-drawn reconstruction of a tree root system based on the analysis of GPR data (Hruska, et al., 1999)

708 Attempts to map tree root systems have continued throughout the years (Sustek, et al.,
709 1999) (Cermak, et al., 2000) (Wielopolski, et al., 2000), with alternate and controversial
710 results. The most significant barrier to mapping complete root systems with GPR is the
711 inability to distinguish individual roots when tight clusters of roots are encountered, as
712 they give one only large parabolic reflection (Butnor, et al., 2001). Furthermore, many
713 pieces of research were carried out under controlled conditions (Barton & Montagu,
714 2004), therefore limiting the significance of the results for in situ tree root mapping.
715 Moreover, the minimum detectable size for tree roots is still a subject of discussion. In
716 fact, tests conducted under controlled conditions confirmed that it was possible to
717 detect fine roots (0.5 cm in diameter or less) (Butnor, et al., 2001), while tests carried
718 out in the field demonstrated that only coarse roots with diameters greater than 5 cm
719 could be identified (Ow & Sim, 2012).

720 Furthermore, research has concentrated on the use of GPR as an appropriate tool for
721 use on valuable trees, or trees in situations where excavation is not possible, such as
722 growing near pavements, roads, buildings or on unstable slopes (Stokes, et al., 2002).
723 GPR data were able to reliably locate roots under pavements and provided a reasonably
724 accurate root count in the compacted soil under concrete (Bassuk, et al., 2011) and
725 asphalt (Cermak, et al., 2000). This is possible thanks to the difference in water content
726 between roots and soil, which can provide the necessary permittivity contrast and
727 therefore allow root detection by GPR (Wielopolski, et al., 2000). Also, it facilitates the
728 distinction between roots and buried utilities (i.e. cables and pipes), which could
729 otherwise generate signal interference, affecting the GPR survey (Ow & Sim, 2012).

730 Another testing issue that has been investigated is the survey methodology. Two
731 experimental sites situated in Italy, subject to different climates and hydrological
732 conditions, were investigated for this purpose (Zenone, et al., 2008). In this study, GPR
733 measurements were taken using antennas of 900 and 1500 MHz applied in square and
734 circular grids (Figure 16): even though square grids are preferable for GPR lines, results
735 obtainable with circular transects (created by rotating the GPR around the tree, keeping
736 a constant radial distance) were tested to ensure a quasi-perpendicular scanning of root

737 systems. The major difficulty in this setup, however, arose from soil unevenness, as it
738 was challenging to push a radar system in circles over roots and stones.

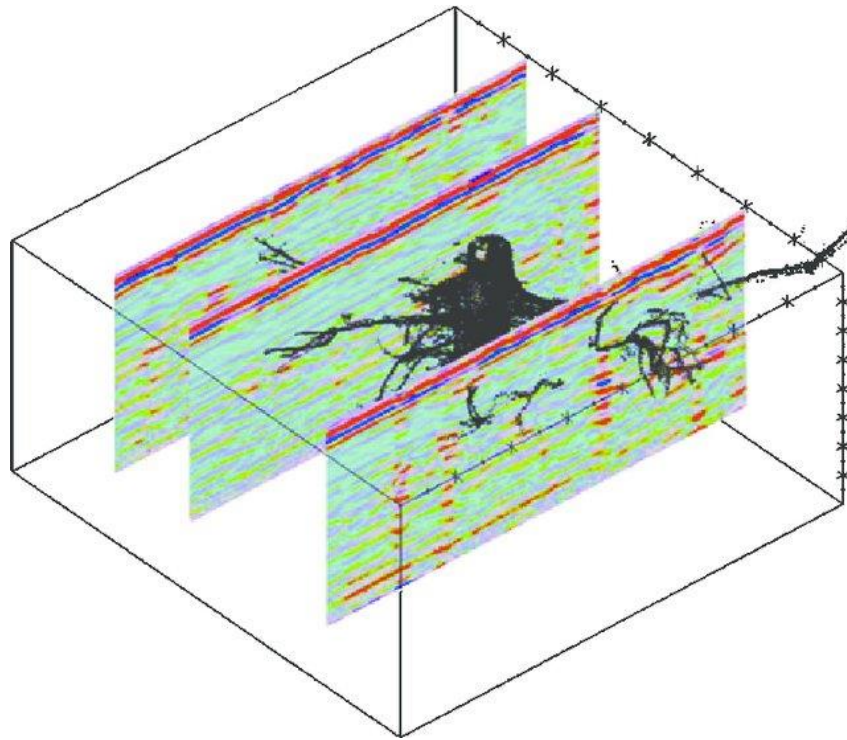


739

740 Figure 16: GPR setups for tree root system survey using a) circular transects and b) square grids (Zenone, et al.,
741 2008)

742 Most of the aforementioned methodologies tested the reliability of their results by
743 digging or uprooting the investigated trees. Zenone, et al. (2008) excavated the root
744 system with an air-spade and pulled it out using a digger; a laser measurement system
745 was then applied in order to create a scan, and the 3D root system architecture was
746 reconstructed.

747 A comparison between the laser scan point cloud and the sections of GPR scans (Figure
748 17) returned a limited grade of correspondence, and the authors stated that this might
749 be due to an alteration of the root system architecture that occurred during the
750 excavation. Nevertheless, the use of GPR for 3D coarse root system architecture
751 reconstruction was further criticised (Guo, et al., 2013).



752

753 **Figure 17: Comparison between 3D rendering from a laser scanner and GPR Bscans (Zenone, et al., 2008)**

754 Set aside the recognition and mapping of tree roots, a challenge that is still object of
755 discussion is the quantification of the biomass of tree roots. As it is widely
756 acknowledged, the estimate of tree root mass density is crucial for the evaluation of the
757 health status of the tree, for the stability of the tree itself and the stability of the soil, as
758 tree roots are used for the reinforcement of slopes. Not least, root mass evaluation is
759 essential for understanding the storage of carbon in the ecosystem (Stover, et al., 2007).

760 Traditional methods for estimating root biomass are usually destructive, time-
761 consuming and expensive, as well as often inaccurate (Birouste, et al., 2014). The
762 application of NDT methods in this research area is still at the early stage, and the
763 achieved results are still not accurate enough (Aulen & Shipley, 2012).

764 GPR has proven to be efficient in the estimation of coarse root biomass (Guo, et al.,
765 2013). Several studies have been conducted so far in field conditions (Butnor, et al.,
766 2001) (Butnor, et al., 2003) (Stover, et al., 2007) (Butnor, et al., 2008) (Samuelson, et al.,
767 2008) (Borden, et al., 2014) and in laboratory environment (Cui, et al., 2011). GPR has
768 shown potential for root quantification, as coarse root biomass has been assessed with

769 reasonably good accuracy (Guo, et al., 2013). However, uncertainty still affects the
770 precision of the existing methodologies. Currently, a limiting factor for a correct root
771 density estimation is the root water content which, if too low, can lead to an
772 underestimation of root biomass (Guo, et al., 2013).

773 In conclusion, all the above-mentioned NDT methods have proven viability in the
774 assessment of tree root systems. However, the knowledge of the application of some of
775 these techniques in tree assessment is still in its infancy. Moreover, their employment
776 can be troublesome, as the required equipment is often difficult to operate. In addition,
777 the application of these methods can often be very expensive. On the other hand, GPR
778 is gaining attention in view of the high versatility, the rapidity of its data collection and
779 the provision of reliable results at relatively limited costs. It has also proven to be a
780 reliable instrument for the assessment of tree root systems. The advantages and
781 limitations of the aforementioned ND techniques in the assessment of tree root systems
782 are summarised in Table 2.

Table 2: Non-destructive testing methods for the assessment of tree root systems

Working principle	Method	Characteristics	Applications	Advantages	Limitations
Imaging	(Mini)Rhizotrons	Non-destructive Slightly invasive	Quantification of fine root growth	<ul style="list-style-type: none"> High-resolution imaging Frequent inspections 	<ul style="list-style-type: none"> Modification of soil hydrology and physics Only small portions of the root system can be observed Disparity in results obtained from different image processing methods Cost of installation Expensive equipment Impossible to install in certain environments (i.e. urban trees)
Mechanical	Pulling test	Non-destructive Invasive	Assessment of tree root plate stability	<ul style="list-style-type: none"> Provides a safety factor for tree stability Test of the elastic response of the tree trunk 	<ul style="list-style-type: none"> Invasive Not completely realistic (i.e. cannot simulate wind effects) Affected by temperature conditions Not useful for understanding the causes of tree instability
Electrical	ERT	Non-destructive Non-invasive	Detection of root distribution Quantification of root biomass	<ul style="list-style-type: none"> Easiness of data collection Suitable for measurements repeated over time Various scales application Possibility of 1D, 2D and 3D surveys Depth of detection 	<ul style="list-style-type: none"> Systematic errors due to poor electrode contact Long measurement times Laboratory calibration phase needed Non-uniqueness of the solution in the inversion scheme Difficult to discern the effect of roots from the background noise for low root biomass
Acoustic	Acoustic detection	Non-destructive Slightly invasive	Detection of roots	<ul style="list-style-type: none"> Successful detection of coarse roots 	<ul style="list-style-type: none"> Small roots (diameter < 4 cm) are not detected Superficial depth of detection (< 50 cm) High sensitivity to water content Difficult to discern roots from other buried objects
Electromagnetic	X-ray CT	Non-destructive Non-invasive	3D mapping of roots Quantification of root length and diameter	<ul style="list-style-type: none"> High-resolution imaging Suitable for measurements repeated over time Detection of fine roots 	<ul style="list-style-type: none"> Difficulty in distinguishing the boundary between roots and other materials High dependence on soil-related factors (i.e. soil type, soil moisture content, presence of organic matter or air-filled pores, root water status) Overestimation of root diameter Underestimation of root length Complex image processing

	GPR	Non-destructive Non-invasive	3D mapping of roots Quantification of root length Dielectric properties measurements	<ul style="list-style-type: none"> • Totally non-invasive • Easy to use • High-resolution imaging • Suitable for measurements repeated over time • Different frequencies for different objectives • Can be used on valuable trees • Capable of finding roots under pavements 	<ul style="list-style-type: none"> • Difficulty of data interpretation • Fine roots are not detected • Impossible to distinguish clusters of roots
--	------------	---------------------------------	--	---	---

784

785 **6. New methodological and data processing prospects for the**
786 **assessment of tree root systems architecture using Ground**
787 **Penetrating Radar: a case study**

788 Recent advances in tree root mapping using GPR have led to the reconstruction of root
789 system geometry using correlation analysis in the 3D domain (Alani, et al., 2018). In this
790 study, two trees of different species, fir and oak, were investigated using circular and
791 semi-circular scanning configurations, in order to test the viability of a novel technique
792 for the creation of a three-dimensional root system model.

793 This study was further developed by Lantini, et al. (2018), with the aim of assessing
794 interactions between different tree root systems. Interconnections between different
795 root systems allow the transmission of pathogenic diseases and fungi. Research into
796 how these roots interact with each other and with the surrounding environment is
797 essential for the achievement of effective containment practices. To achieve this aim,
798 this pilot research study focused on the estimate of root mass density, and this objective
799 was addressed by evaluating the total root length per reference unit. Promising results
800 were obtained, demonstrating that local increases in density occur in the area where
801 interconnections are supposed to happen.

802 Further research, which includes advanced signal processing, is now under
803 development, with the aim of reducing uncertainty and false alarms in root detection.
804 To this extent, a case study is presented, in which a dedicated data processing
805 methodology, based on three main chronological stages, is applied to GPR data. An
806 improved pre-processing algorithm is proposed, with the aim of reducing clutter in raw
807 GPR data, improve target detection and increase deeper reflections which are likely to
808 be related to deep root systems but have been attenuated due to increasing depths or
809 highly conductive materials. Furthermore, advanced signal processing techniques are
810 applied, in an effort to remove ringing noise from GPR data and focus on the response
811 from the target. Subsequently, an iterative procedure for tree root recognition and
812 tracking and root system architecture reconstruction in a 3D domain is implemented,
813 based on a correlation analysis between identified targets. Lastly, the domain is divided

814 into reference volume units and root density maps are produced. This approach has
815 given promising results, proving that GPR has the potential to identify both the shallow
816 (within the first 25 cm of soil) and the deep (more than 25 cm from the soil surface) root
817 systems, and find viable root paths, allowing for the construction of three-dimensional
818 models of root systems for different species of trees.

819 **6.1. Materials and methods**

820 **6.1.1. The survey technique**

821 The survey was carried out in Walpole Park, Ealing, London (United Kingdom). The soil
822 around a mature tree (trunk circumference at ground level of 3.83 m and radius of 0.61
823 m) was investigated (Figure 18). 24 circular scans were performed on the soil around the
824 tree trunk, starting 0.50 m from the bark and then 0.30 m apart from one another. Thus,
825 an overall area of 197.69 m² was examined.



826

827

828

Figure 18: The investigated area

829 **6.1.2. The GPR equipment**

830 The survey was performed using a ground-coupled GPR system (Opera Duo, IDS
831 GeoRadar (Part of Hexagon)), equipped with 700 MHz and 250 MHz central frequency
832 antennas (Figure 19). Data acquisition was performed using a time window of 80 ns and
833 512 samples. The horizontal resolution was set to 3.2×10^{-2} m. For this study, only data
834 from the 700 MHz frequency antenna were analysed, as these provide the highest
835 effective resolution (Benedetto, et al., 2011) (Benedetto, et al., 2013).



836

837

838

Figure 19: Opera Duo GPR system

839 **6.1.3. Signal processing methodology**

840 As previously stated, the data processing methodology is divided into three main stages.
841 A pre-processing stage was envisaged, aiming to eliminate clutter-related signal and
842 increase the signal-to-noise ratio (SNR). To this purpose, advanced signal processing
843 techniques were implemented. Moreover, in order to achieve information about the
844 architecture of the entire tree root system, reflections from deeply localised targets
845 were amplified.

846 **6.1.3.1. Pre-processing stage**

847 The need for a pre-processing stage arises from the fact that raw GPR data are often
848 corrupted by clutter. This can make the data interpretation difficult, as the response
849 from the real targets can be disguised. In order to ensure the widest possible
850 applicability of the proposed methodology, basic signal processing techniques were
851 considered. Thus, a sequential use of a) zero-offset removal, b) zero correction, c)
852 bandpass filtering and d) time-varying gain was performed.

853 Nevertheless, the application of the aforementioned techniques does not help with the
854 removal of ringing noise, which is a repetitive type of clutter and can appear as
855 horizontal and periodic events. When present, ringing noise can conceal the real target
856 of the investigation, with resulting misinterpretation of results. One of the most
857 effective techniques for ringing noise removal, the Singular Value Decomposition (SVD),
858 was therefore implemented in this stage.

859 The concept behind the SVD filter is that a GPR image can be divided into several sub-
860 images (eigenimages), each of which contains some of the information relating to the
861 original image. Since components such as ringing noise are highly correlated, it is
862 possible to separate their response from the one given by the real target of the
863 investigation, thus eliminating the clutter to enhance the SNR.

864 Another important advancement in the signal processing stage arises from the need to
865 have information on the real position of the target. As previously stated, the response
866 from a target in a GPR survey is given by a reflection hyperbola, the apex of which
867 corresponds to the position of the buried object. This concept is acceptable for a simple

868 location of a target. However, automatic mapping of a tree root system architecture in
869 a 3D domain requires the target to be concentrated in a single point. This will avoid false
870 alarms for root identification. To this effect, a frequency-wavenumber (F-K) migration
871 was applied to GPR data, assuming a constant velocity of the medium and estimating it
872 through an iterative procedure. This allowed to find the permittivity value that best fit
873 the data.

874 **6.1.3.2. Tree root tracking algorithm**

875 The implementation of the algorithm for the automatic reconstruction of the tree root
876 system geometry consists of two main parts. In the first part, the main settings, based
877 on fundamental set up hypotheses, are defined (i.e. the outcomes of the previous pre-
878 processing phase, matrix dimensions, and GPR data acquisition settings). In addition,
879 other important variables (i.e. the data acquisition method and the dielectric properties
880 of the medium) are initialised.

881 Subsequently, the pre-processed GPR data undergo an iterative procedure, in order to
882 find a correlation between the amplitude values in different positions of the 3D domain.
883 The steps of the procedure are the following:

- 884 • *Detection of the target*: each amplitude value in the data matrix is compared with
885 a predefined threshold value, in order to identify the reflections that are more
886 likely to belong to tree roots.
- 887 • *Correlation analysis*: a spatial correlation analysis is carried out between the
888 identified reflections.
- 889 • *Root tracking*: where a correlation is found, targets are assembled into vectors
890 which represent the spatial coordinates of the identified root.
- 891 • *Reconstruction of root system architecture in the 3-D domain*: all the vectors are
892 positioned in a 3D environment, based on the previously identified coordinates,
893 to recreate a rendering of the tree root system.

894

895 **6.1.3.3. Root density evaluation**

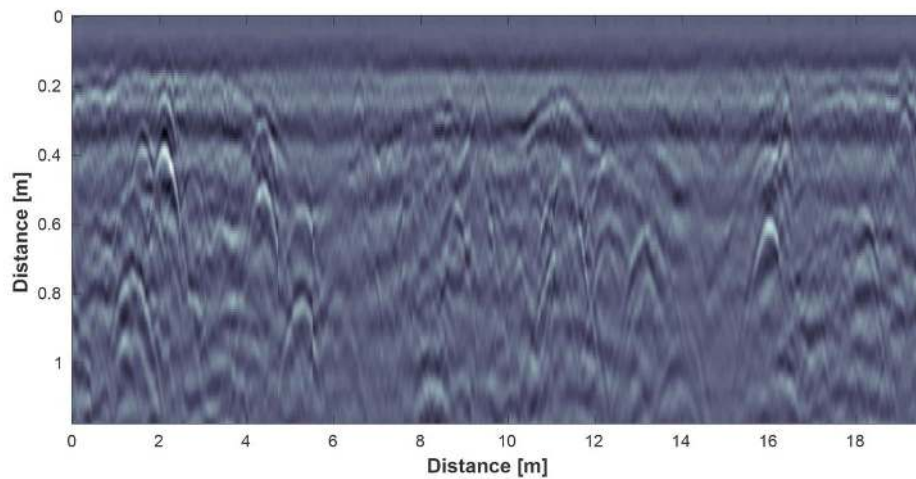
896 In this final step, root density is evaluated based on the position and length of the roots
897 obtained in the previous phase. Through the application of a polynomial fitting function,
898 the roots' path was better approximated in a continuous domain, thus allowing for the
899 estimation of the length of each root. Based on this, the volume in which the tree root
900 system resides was divided into reference volumes, and the length of the roots enclosed
901 in each volume was evaluated as follows:

$$d = \frac{\sum_{i=1}^n L_i}{V} \quad (6)$$

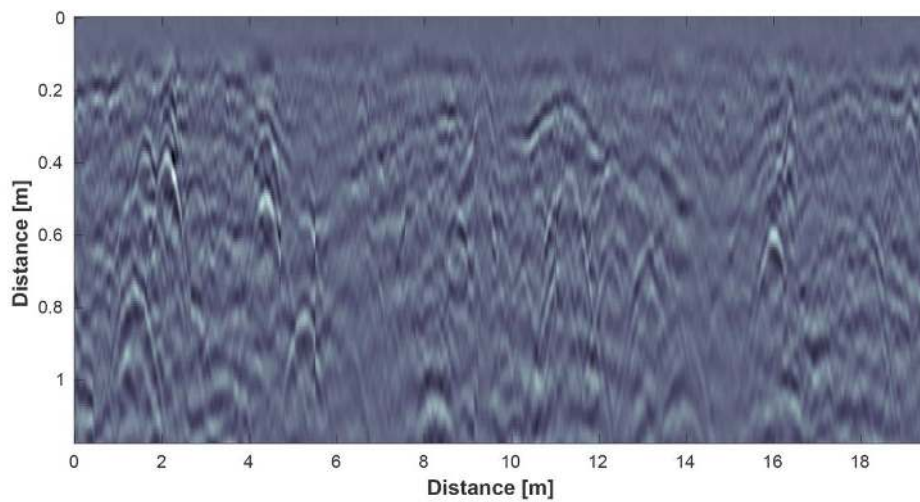
902 where d is the density [m/m^3], n is the number of roots contained in a reference unit of
903 volume [m^3] and L_i is the length of the root [m].

904 **6.1.4. Results and discussion**

905 The advances made here to the GPR data pre-processing phase have allowed a more
906 effective identification of the tree roots, significantly reducing the margin of error. In
907 fact, they made it possible to remove horizontal layers and repeated reflections given
908 by ringing noise through the application of the SVD filter. Figure 20 shows an example
909 of B-scan before (a) and after (b) the application of the SVD filter, from the analysis of
910 which it is clear that the effect of noise-related features is considerably mitigated.



(a)



(b)

911

912

Figure 20: Bscan before (a) and after (b) the application of the SVD filter

913

914

915

916

917

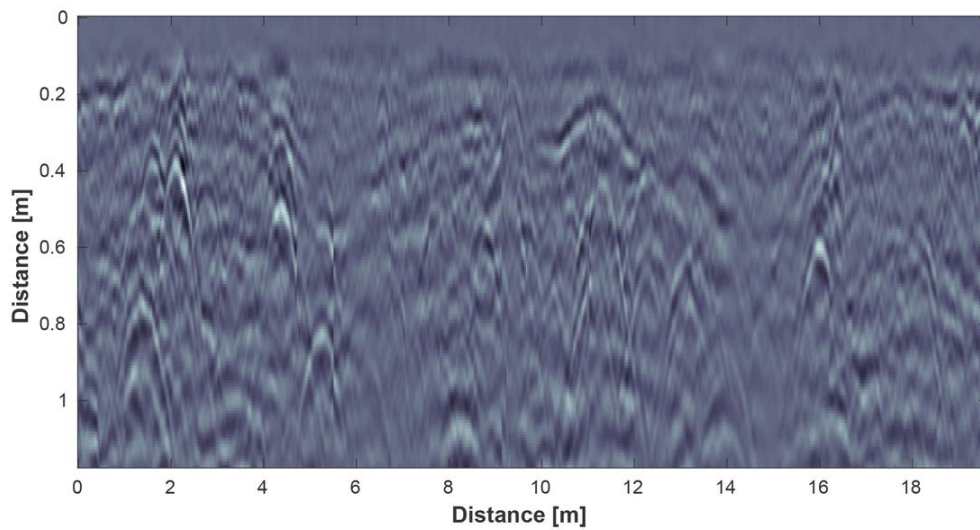
918

919

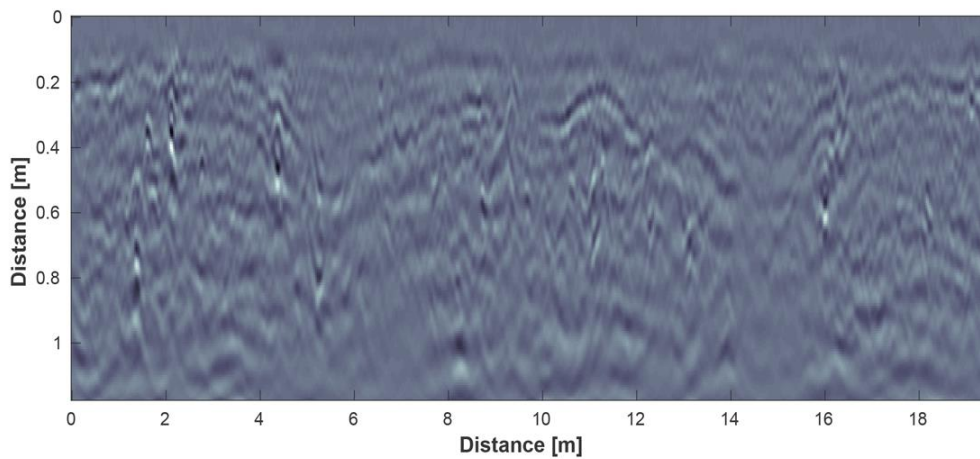
920

921

Moreover, the application of F-K migration significantly improved the effectiveness of the subsequent phases of the algorithm, as the margin of error in identifying the true position of the roots was significantly reduced. In fact, the tails of the hyperbole made accurate target detection difficult, as not infrequently points far from the apices (i.e. the real location of the target) were higher than the set threshold. Thus, the migration process increased the reliability of the subsequent steps. Figure 21 shows a comparison between a B-scan before (a) and after (b) the application of the F-K migration. It is evident how the hyperbolic response of the targets has become a single focused point, which corresponds to the target's real position.



(a)



(b)

922

923

Figure 21: Bscan before (a) and after (b) the application of F-K migration

924

Subsequently, the application of the root tracking algorithm to the processed data

925

allowed for the reconstruction of the tree root system architecture in a three-

926

dimensional environment. Figure 22 shows the result of this procedure in a 2D planar

927

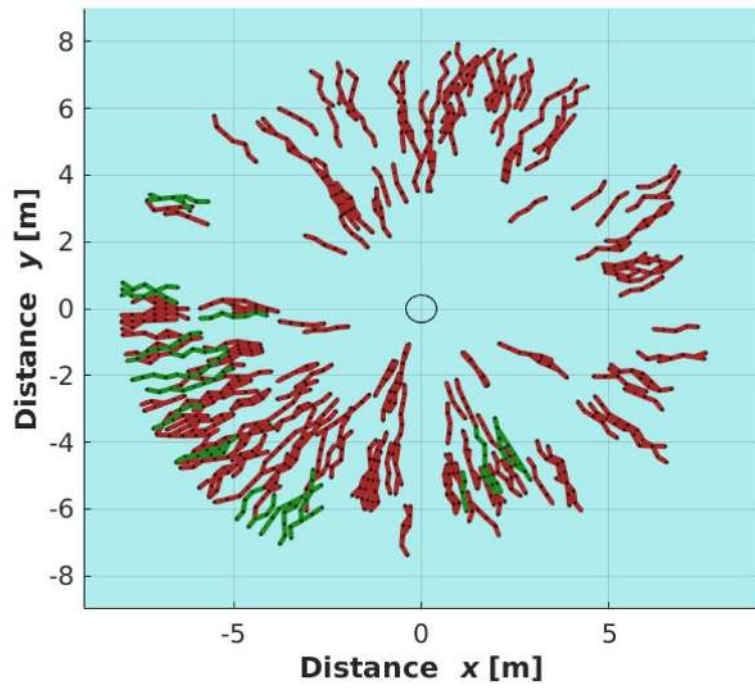
view (a) and in a 3D environment (b). To make interpreting the results easier, shallow-

928

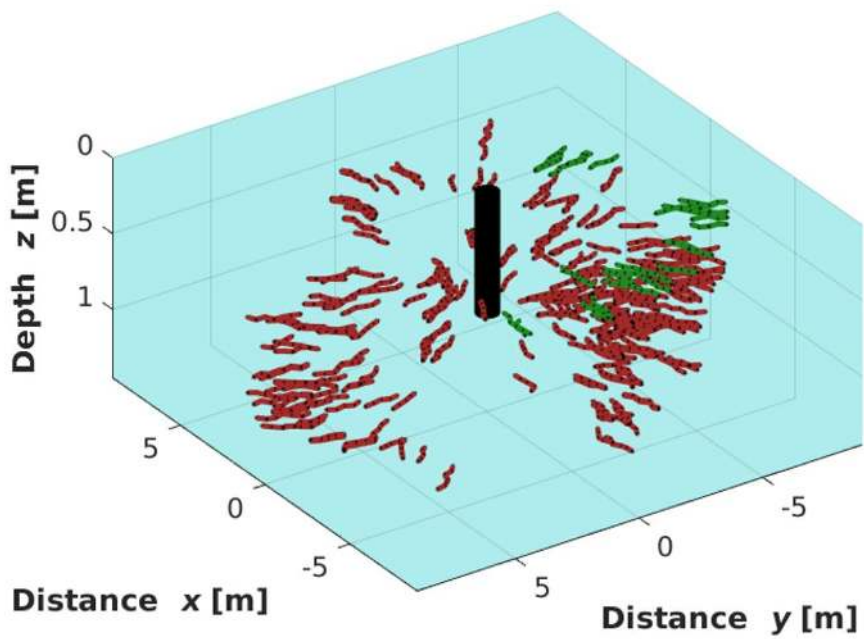
buried roots (i.e. within the first 25 cm of soil) have been represented with a different

929

colour than deeper roots.



(a)



(b)

930

931

Figure 22: 2D planar view (a) and 3D rendering (b) of the investigated root system

932 Results have proven the potential of the algorithm in identifying consistent root paths.
933 Points belonging to the roots were successfully identified and linked together, based on
934 a spatial correlation analysis.

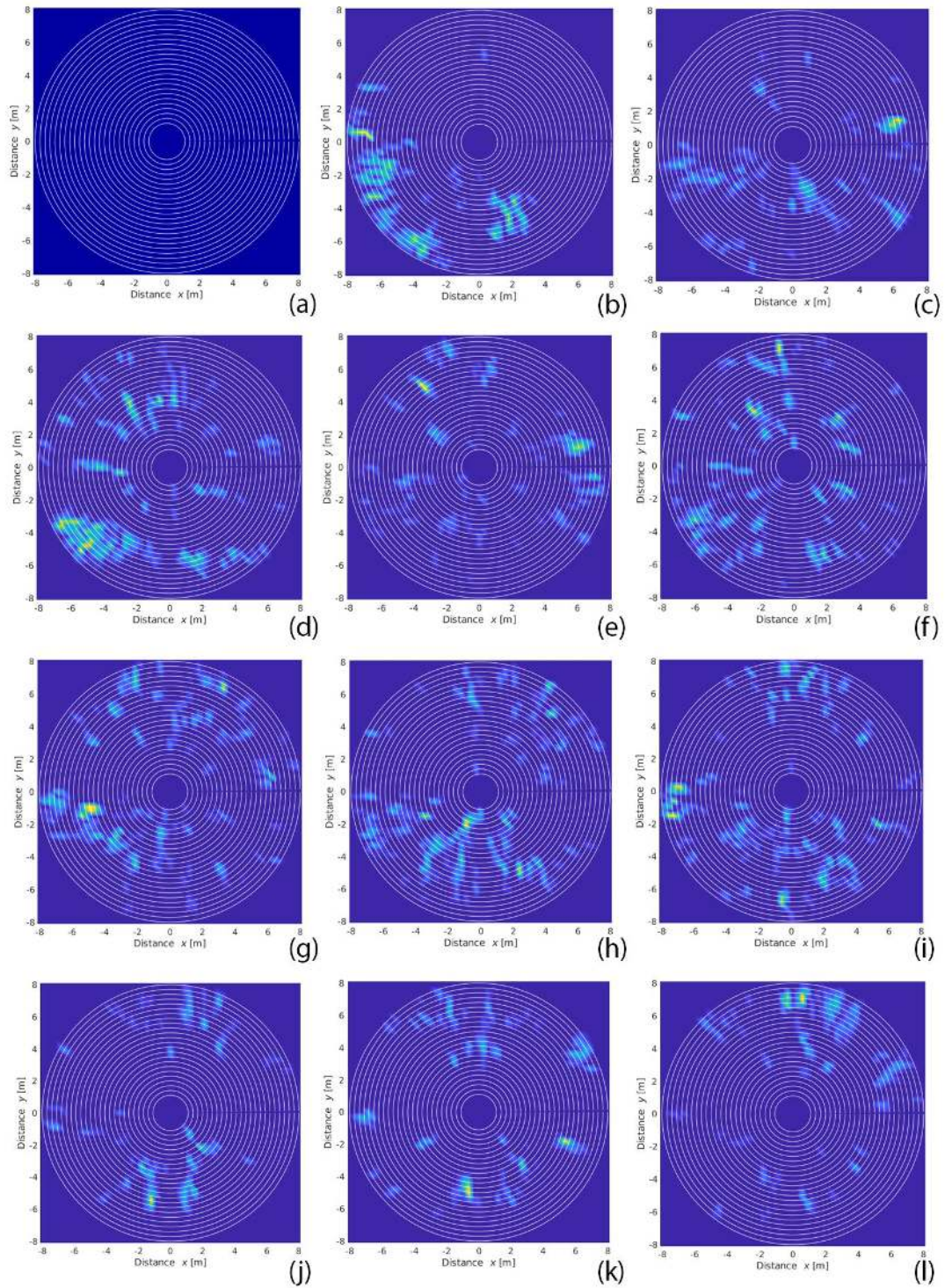
935 From the analysis of B-scans, the strongest reflections resulted to be located within the
936 first 80 cm of soil. Nevertheless, the application of the time-varying gain function
937 allowed the detection of deeper targets, up to a maximum depth of 1.20 m. This result
938 is in line with what was expected, as generally tree root systems develop in the first 2 m
939 of subsoil, with the 90% to the 99% of roots occurring in the first meter (Crow, 2005).

940 As depicted in Figure 22, root discontinuity is visible in certain areas. Possible
941 explanations for this could be:

- 942 • Presence of a higher moisture content (Ortuani, et al., 2013) or a high
943 concentration of clay in certain areas of subsoil (Patriarca, et al. 2013; Tosti, et
944 al., 2016).
- 945 • Propagation of tree roots vertically downwards within the soil matrix

946 Furthermore, in order to avoid the inclusion of non-root targets within the soil (cobles
947 and utility futures), the algorithm is programmed to discard shorter roots.

948 The architecture of the root system was then further investigated through the
949 evaluation of root density at different depths, using the proposed equation (Equation
950 6). The domain investigated was divided into reference volumes of 0.3 m × 0.3 m × 0.1
951 m and thus analysed to determine the total root length per reference unit. Figure 23
952 presents the outcomes of this data processing stage. Several areas with a high density
953 of roots can be identified, as shown in Table 3.



954

955 **Figure 23: GPR-derived root density maps, related to the following depths: a) from 0 m to 0.10 m; b) from 0.10 m**
 956 **to 0.20 m; c) from 0.20 m to 0.30 m; d) from 0.30 m to 0.40 m; e) from 0.40 m to 0.50 m; f) from 0.50 m to 0.60 m;**
 957 **g) from 0.60 m to 0.70 m; h) from 0.70 m to 0.80 m; i) from 0.80 m to 0.90 m; j) from 0.90 m to 1.00 m; k) from**
 958 **1.00 m to 1.10 m; l) from 1.10 m to 1.20 m;**

Table 3: Zones of increased root density for the investigated tree

Zones of increased density					
Depth [m]	x		y		Maximum values [m/m ³]
	From [m]	To [m]	From [m]	To [m]	
0.10 - 0.20	-6.30	-7.20	0.00	0.60	1.25
	-6.30	-6.60	-3.30	-3.60	1.08
	2.10	2.40	-3.60	-3.90	1.03
0.20 - 0.30	5.70	6.90	0.90	1.50	2.05
	0.60	1.20	-2.40	-3.00	1.14
	6.30	6.60	-4.20	-4.50	1.11
	-6.30	-6.60	-1.20	-1.50	1.11
	-4.20	-4.50	-2.10	-2.40	1.11
	0.00	0.30	-3.60	-3.90	1.05
0.30 - 0.40	-2.40	-6.90	-3.30	-5.70	1.85
	-0.60	0.60	3.90	4.20	1.55
	-1.80	-2.40	3.00	3.90	1.49
	-2.70	-4.20	0.00	-0.60	1.48
	0.90	2.10	-5.40	-6.00	1.28
	-6.30	-6.60	2.70	3.00	1.11
0.40 - 0.50	-3.00	-3.60	4.50	5.10	2.49
	5.40	6.90	0.60	1.80	1.84
	6.90	7.50	-0.60	-1.80	1.50
	-1.50	-1.80	6.60	6.90	1.20
	-2.40	-2.70	1.80	2.10	1.09
0.50 - 0.60	-0.60	-0.90	6.60	7.50	1.88
	-2.10	-2.70	3.00	3.60	1.79
	2.40	3.00	2.40	3.00	1.67
	-5.70	-6.00	-3.30	-4.50	1.48
	1.80	2.10	-5.40	-5.70	1.33
	3.30	3.60	-1.50	-1.80	1.33
	3.00	3.30	0.90	1.20	1.32
	-1.80	-2.10	-3.60	-3.90	1.12
	1.50	1.80	-1.80	-2.10	1.05
	-3.60	-3.90	-3.30	-3.60	1.04
-6.60	-6.90	2.70	3.00	1.00	
0.60 - 0.70	-4.20	-5.40	-0.90	-1.80	2.20
	3.30	3.60	6.00	6.60	1.94
	-2.70	-4.50	-2.40	-3.30	1.66
	-1.80	-2.10	-4.20	-4.80	1.53
	-1.80	-2.10	6.30	7.20	1.48
	6.30	6.60	0.60	0.90	1.46
	-3.00	-3.60	4.50	5.10	1.26
	-6.60	-7.50	0.00	-0.90	1.17
	-0.30	-0.60	-2.40	-3.00	1.15
	-1.80	-2.10	3.30	3.60	1.04
0.70 - 0.80	-0.30	-3.60	-1.50	-5.10	2.25

	2.40	2.70	-4.50	-5.40	1.94
	1.50	1.80	-1.80	-2.10	1.60
	4.20	4.80	4.50	4.80	1.55
	4.20	4.50	6.00	6.60	1.49
	1.50	1.80	-4.80	-5.10	1.33
	3.60	3.90	-4.50	-4.80	1.33
	-5.10	-5.40	-1.20	-1.50	1.29
	0.00	-0.60	5.10	6.00	1.18
	4.80	5.10	2.40	2.70	1.06
	-6.60	-6.90	-0.30	-0.60	1.05
	-6.30	-6.90	-2.40	-3.60	1.04
0.80 - 0.90	-6.60	-7.50	0.30	-1.80	1.74
	-0.30	-0.60	-6.60	-7.20	1.36
	5.40	5.70	-2.10	-2.40	1.27
	0.90	1.50	6.60	7.20	1.21
	4.50	4.80	3.00	3.30	1.16
	0.00	-0.30	7.20	7.50	1.14
	1.80	2.10	-5.40	-5.70	1.10
	0.00	-0.30	-1.50	-1.80	1.03
0.90 - 1.00	-0.90	-1.80	-3.30	-6.00	2.22
	1.20	2.10	-1.20	-5.40	1.65
	3.00	3.30	6.60	6.90	1.24
	2.10	2.40	5.10	5.70	1.20
	3.00	3.30	3.90	4.20	1.06
1.00 - 1.10	5.10	6.00	-1.80	-2.10	2.43
	-0.30	-0.90	-4.20	-5.40	2.25
	2.70	3.00	-3.00	-3.60	1.64
	0.30	0.60	3.60	4.20	1.39
	-3.00	-3.60	-1.80	-2.40	1.39
	6.00	6.90	3.30	3.90	1.27
	-1.50	-1.80	5.70	6.60	1.26
	-6.30	-7.20	-0.30	-0.60	1.19
	1.50	1.80	-1.80	-2.10	1.13
-1.20	-1.50	2.70	3.30	1.11	
1.10 - 1.20	-0.60	1.20	6.30	7.20	2.29
	2.40	2.70	5.70	6.90	1.26
	0.60	0.90	4.20	4.50	1.24
	3.90	4.20	-3.30	-3.60	1.15
	2.10	2.40	2.70	3.00	1.03

960 From the analysis of the results, it can be noticed that there is a high density of roots in
961 the south-west quadrant, at a depth between 0.10 m and 1.10 m. This result could be
962 due to the peculiar location of the investigated tree in the park. In fact, the tree is
963 confined to the north by the presence of a pathway, which requires a higher compaction
964 level than the undisturbed soil. Moreover, root development is not limited to the south-

965 west direction, as there are no other trees which could compete for the exploitation of
966 soil resources. Nevertheless, we can note the presence of areas of high root density in
967 the east direction, between 0.30 m and 0.50 m deep and at a great distance from the
968 trunk. This could be due to the close proximity of another tree, which roots are
969 interconnected with the ones of the investigated system. In fact, in that direction root
970 density gradually decreases, to then increase again towards the limit of the surveyed
971 area, bordering the area potentially affected by the roots of the adjacent tree. Such an
972 outcome is in line with the results provided by Lantini, et al. (2018).

973 The evaluation of tree root density in soil has therefore proven to be an effective tool
974 for the assessment of the root system conditions. Variations in time of root density,
975 obtained by repeating GPR tests at appropriate intervals, could help in the assessment
976 of the root system health. In fact, sudden reductions in root density could be due to the
977 occurrence of diseases or fungal attacks. Thus, acknowledging the problem at its early
978 stage could allow the application of appropriate remedial actions, in order to save the
979 tree and prevent infection from spreading to other trees.

980

981 **7. Conclusion**

982 In this review paper, the authors have presented a significant proportion of the existing
983 literature within the subject area of assessment and monitoring of tree roots and their
984 interaction with the soil. To that effect the nature of tree root systems, their architecture
985 and the factors affecting their development have been covered. Emphasis was paid to
986 establishing the reasons behind the increasing importance of assessment and health
987 monitoring of tree roots and their relationship with the health of trees.

988 An emphasis is given to the major destructive methods for tree root detection and
989 mapping, followed by a section presenting a summary of the main non-destructive
990 testing methods and the research outputs based on their application for tree root
991 system evaluation. The paper also clearly demonstrated that the investigation of tree
992 root systems using non-destructive testing (NDT) methods is effective and is gaining
993 momentum. As the awareness of the importance of the world's natural heritage is
994 growing, hopefully more desperately needed research and development work will be
995 carried out and efforts will be devoted to this vitally important area of endeavour.

996 Due to its ease of use, its non-intrusiveness nature and its relatively low costs, Ground
997 Penetrating Radar (GPR) was found to be one of the most reliable tools for root
998 inspection. Recent research has focused on root detection and three-dimensional
999 mapping of tree root systems architecture and root diameter, and the evaluation of root
1000 diameter in complex urban areas. New research is now focusing on tree root and soil
1001 interactions, as well as the interconnectivity of tree roots with one another.
1002 Furthermore, it is important to report that the authors are currently engaged with
1003 research involving novel survey methodologies and data acquisition techniques which
1004 in turn have been applied in assessing a variety of tree species. Promising results have
1005 been obtained within the context of tree roots variations as well as the soil
1006 characterisations.

1007 Advancements in GPR signal processing for tree root assessment and mapping are also
1008 under development. To that effect, a case study was presented, focusing on the removal

1009 of noise-related information for an improved automatic recognition and mapping of tree
1010 roots in a 3D environment.

1011 Regarding the assessment of the root mass density, it is important to conclude that, at
1012 the present time, existing assessment methods are unable to provide accurate
1013 estimations. As has been pointed out earlier, the importance of assessing tree root
1014 density is vital for several purposes, ranging from the health of the tree to the safety of
1015 the surrounding environment (including buildings and infrastructure). It was noted that
1016 a definitive approach is difficult to achieve, as the estimation of root density is an
1017 indirect output of the compiled GPR data. Within this framework, the authors have
1018 proposed a new emerging approach, based on the evaluation of a novel root density
1019 index. Root density is evaluated based on the position and length of the roots, as it is
1020 obtained from the modelling phase of the root mapping algorithm. Results have given
1021 encouraging outcomes, showing that a more reliable estimation of tree root density can
1022 be achieved. More research is now under development, in order to demonstrate the
1023 viability of the proposed algorithm. To this extent, tests on several species of trees, using
1024 different antenna systems (frequencies and type) and survey conditions, are under
1025 development.

1026 **8. Acknowledgements**

1027 This paper is dedicated to the memory of Jonathan West; a friend, a colleague, a
1028 forester, a conservationist and an environmentalist, who died following an accident in
1029 the woodland that he loved.

1030 We would like to thank The Lord Faringdon Charitable Trust and The Schroder
1031 Foundation for supporting this project.

1032 **9. References**

- 1033 al Hagrey, S. A., 2007. Geophysical imaging of root-zone, trunk, and moisture
1034 heterogeneity. *Journal of Experimental Botany*, Volume 58, pp. 839-854.
- 1035 Alani, A. M., Aboutalebi, M. & Kilic, G., 2013. Applications of ground penetrating radar
1036 (GPR) in bridge deck monitoring and assessment. *Journal of Applied Geophysics*, Volume
1037 97, pp. 45-54.
- 1038 Alani, A. M. et al., 2018. *Mapping the root system of matured trees using ground*
1039 *penetrating radar*. s.l., IEEE, pp. 1-6.
- 1040 Alani, A. M. & Tosti, F., 2018. GPR applications in structural detailing of a major tunnel
1041 using different frequency antenna systems. *Construction and Building Materials*,
1042 Volume 158, pp. 1111-1122.
- 1043 Amato, A. et al., 2009. Multi - electrode 3D resistivity imaging of alfalfa root zone.
1044 *European Journal of Agronomy*, Volume 31, pp. 213-222.
- 1045 Amato, M. et al., 2008. In situ detection of tree root distribution and biomass by multi -
1046 electrode resistivity imaging. *Tree Physiology*, Volume 28, pp. 1441-1448.
- 1047 Amato, M. & Ritchie, J. T., 2002. Spatial Distribution of Roots and Water Uptake of Maize
1048 (*Zea mays* L.) as Affected by Soil Structure. *Crop Science*, Volume 42, pp. 773-780.
- 1049 Anagnostakis, S. L., 1987. Chestnut blight: the classical problem of an introduced
1050 pathogen. *Mycologia*, 79(1), pp. 23-37.
- 1051 Aukema, J. E. et al., 2011. Economic impacts of non-native forest insects in the
1052 continental United States. *PLoS One*, 6(9).
- 1053 Aulen, M. & Shipley, B., 2012. Non-destructive estimation of root mass using electrical
1054 capacitance on ten herbaceous species. *Plant and Soil*, 355(1-2), pp. 41-49.
- 1055 Barker, P. A., 1983. *Some urban trees of California: maintenance problems and genetic*
1056 *improvement possibilities*. s.l., s.n., pp. 47-54.

1057 Barton, C. V. M. & Montagu, K. D., 2004. Detection of tree roots and determination of
1058 root diameters by ground penetrating radar under optimal conditions. *Tree Physiology*,
1059 Volume 24, pp. 1323-1331.

1060 Basso, B. et al., 2010. Two-Dimensional Spatial and Temporal Variation of Soil Physical
1061 Properties in Tillage Systems Using Electrical Resistivity Tomography. *Agronomy Journal*,
1062 Volume 102.

1063 Bassuk, N., Grabosky, J., Mucciardi, A. & Raffel, G., 2011. Ground-penetrating Radar
1064 Accurately Locates Tree Roots in Two Soil Media Under Pavement. *Arboriculture &*
1065 *Urban Forestry*, Volume 37, pp. 160-166.

1066 Benedetto, A. et al., 2017. Railway ballast condition assessment using ground-
1067 penetrating radar – An experimental, numerical simulation and modelling development.
1068 *Construction and Building Material*, Volume 140, pp. 508-520.

1069 Benedetto, A., Tosti, F., Bianchini Ciampoli, L. & D'Amico, F., 2017. An overview of
1070 ground-penetrating radar signal processing techniques for road inspections. *Signal*
1071 *Processing*, Volume 132, pp. 201-209.

1072 Benedetto, A. et al., 2013. *Soil moisture mapping using GPR for pavement applications*.
1073 s.l., IWAGPR 2013 - Proceedings of the 2013 7th International Workshop on Advanced
1074 Ground Penetrating Radar.

1075 Benedetto, A. et al., 2015. Mapping the spatial variation of soil moisture at the large
1076 scale using GPR for pavement applications. *Near Surface Geophysics*, 13(3), pp. 269-278.

1077 Benedetto, A., Tosti, F., Schettini, G. & Twizere, C., 2011. *Evaluation of geotechnical*
1078 *stability of road using GPR*. s.l., 2011 6th International Workshop on Advanced Ground
1079 Penetrating Radar (IWAGPR 2011).

1080 Besson, A. et al., 2004. Structural heterogeneity of the soil tilled layer as characterized
1081 by 2D electrical resistivity surveying. *Soil & Tillage Research*, Volume 79, pp. 239-249.

- 1082 Bianchini Ciampoli, L., Tosti, F., Economou, N. & Benedetto, F., 2019. Signal Processing
1083 of GPR Data for Road Surveys. *Geosciences*, 9(96).
- 1084 Biddle, G., 2001. Tree root damage to buildings. In: C. Vipulanandan, M. B. Addison & M.
1085 Hasen, eds. *Expansive Clay Soils and Vegetative Influence on Shallow Foundations*.
1086 s.l.:s.n., pp. 1-23.
- 1087 Birouste, M. et al., 2014. Measurement of fine root tissue density: a comparison of three
1088 methods reveals the potential of root dry matter content. *Plant and Soil*, 374(1-2), pp.
1089 299-313.
- 1090 Blunt, S. M., 2008. Trees and pavements - are they compatible?. *Arboricultural Journal*,
1091 Volume 31, pp. 73-80.
- 1092 Bohm, W., 2012. *Methods of studying root systems*. s.l.:Springer Science & Business
1093 Media.
- 1094 Bonan, G. B., 1992. Soil temperature as an ecological factor in boreal forests. In: H. H.
1095 Shugart, R. Leemans & G. B. Bonan, eds. *A Systems Analysis of the Global Boreal Forest*.
1096 s.l.:Cambridge University Press, pp. 126-143.
- 1097 Borden, K. A. et al., 2014. Estimating coarse root biomass with ground penetrating radar
1098 in a tree-based intercropping system. *Agroforestry Systems*, 88(4), pp. 657-669.
- 1099 Boyer, J. S., 1995. Roots and root systems. In: *Water relations of plants and soils*.
1100 s.l.:Academic Press, Inc..
- 1101 Brennan, G., Patch, D. & Stevens, F. R. W., 1997. *Tree Roots and Underground Pipes -*
1102 *Arboriculture Research Note*, s.l.: Arboricultural Advisory & Information Service.
- 1103 Brudi, E. & Wassenauer, P., 2002. *Trees and Statics: Non-Destructive Failure Analysis*.
1104 Champaign, Illinois, International Society of Arboriculture, pp. 53-70.
- 1105 Bucur, V., 2006. *Acoustics of wood*. s.l.:Springer Science & Business Media.

- 1106 Butnor, J. R. et al., 2003. Utility of Ground-Penetrating Radar as a Root Biomass Survey
1107 Tool in Forest Systems. *Soil Science Society of America Journal*, Volume 67, pp. 1607-
1108 1615.
- 1109 Butnor, J. R. et al., 2001. Use of ground-penetrating radar to study tree roots in the
1110 southeastern United States. *Tree Physiology*, Volume 21, pp. 1269-1278.
- 1111 Butnor, J. R. et al., 2008. Using Ground-Penetrating Radar to Estimate Tree Root Mass
1112 Comparing Results from Two Florida Surveys. In: B. J. Allred, J. J. Daniels & M. R. Ehsami,
1113 eds. *Handbook of Agricultural Geophysics*. Boca Raton: CRC Press, pp. 375-382.
- 1114 Buza, A. K. & Divos, F., 2016. Root stability evaluation with non - destructive techniques.
1115 *Acta Silvatica et Lignaria Hungarica*, Volume 12, pp. 125-134.
- 1116 Buza, A. K. & Goncz, B., 2015. Comparison of trees and NDT methods. *Wood research*,
1117 Volume 60, pp. 45-58.
- 1118 Canadian Forest Service, 2015. *Trees, insects and diseases of Canada's forests - Natural*
1119 *Resources* *Canada*. [Online]
1120 Available at: <https://tidcf.nrcan.gc.ca/en/diseases/factsheet/16>
- 1121 Caneva, G., Ceschin, S. & De Marco, G., 2006. Mapping the risk of damage from tree
1122 roots for the conservation of archaeological sites: the case of the Domus Aurea, Rome.
1123 *Conservation and Management of Archaeological Sites*, pp. 163-170.
- 1124 Caneva, G., Galotta, G., Cancellieri, L. & Savo, V., 2009. Tree roots and damages in the
1125 Jewish catacombs of Villa Torlonia (Roma). *Journal of Cultural Heritage*, pp. 53-62.
- 1126 Cermak, J., Hruska, J., Martinkova, M. & Prax, A., 2000. Urban tree root systems and
1127 their survival near houses analyzed using ground penetrating radar and sap flow
1128 techniques. *Plant and Soil*, Volume 219, pp. 103-116.
- 1129 Conyers, L. B., 2002. Ground penetrating radar. *Encyclopedia of Imaging Science and*
1130 *Technology*.

- 1131 Costello, L. R. & Jones, K. S., 2003. *Reducing infrastructure damage by tree roots: a*
1132 *compendium of strategies*. s.l.:Western Chapter of the International Society of
1133 Arboriculture (WCISA).
- 1134 Coutts, M. P., 1983. Root architecture and tree stability. *Plant and Soil*, pp. 171-188.
- 1135 Crow, P., 2005. *The influence of soils and species on tree root depth*. Edinburgh: Forestry
1136 commission.
- 1137 Cui, X. H. et al., 2011. Modeling tree root diameter and biomass by ground-penetrating
1138 radar. *Science China Earth Sciences*, 54(5), pp. 711-719.
- 1139 Cutler, D. & Richardson, I. B. K., 1981. Tree roots and buildings. *Construction Press*.
- 1140 Daniels, D. J., 1996. Surface - penetrating radar. *Electronics & Communication*
1141 *Engineering Journal*, pp. 165-182.
- 1142 Daniels, D. J., 2004. *Ground Penetrating Radar*. s.l.:let.
- 1143 Day, R. W., 1991. Damage of structures due to tree roots. *Journal of Performance of*
1144 *Constructed Facilities*, pp. 200-207.
- 1145 Divos, F., Bejo, L. & Toth, A., 2009. *Instrument supported tree evaluation in Hungary*.
1146 Beijing, Beijing Forestry University, pp. 71-76.
- 1147 Driscoll, R., 1983. The influence of vegetation on the swelling and shrinking of clay soils
1148 in Britain. *Geotechnique* , pp. 93-105.
- 1149 Eshel, A. & Beeckman, T., 2013. *Plant roots: the hidden half*. 3rd ed. ed. New York: Marcel
1150 Dekker.
- 1151 Fay, N., 2014. *Appraisal of Trees at Walpole Park*, London: s.n.
- 1152 Francis, J. K., Parresol, B. R. & de Patino, J. M., 1996. Probability of Damage to Sidewalks
1153 and Curbs by Street Trees in the Tropics. *Journal of Arboriculture*, Volume 22.

- 1154 Gibbs, J. N., 1978. Intercontinental epidemiology of Dutch elm disease. *Annual Review*
1155 *of Phytopathology*, 16(1), pp. 287-307.
- 1156 Goodman, D., 1994. Ground - penetrating radar simulation in engineering and
1157 archaeology. *Geophysics*, Volume 2, pp. 224-232.
- 1158 Grabianowski, M., Manley, B. & Walker, J. C. F., 2006. Acoustic measurements on
1159 standing trees, logs and green lumber. *Wood Science and Technology*, 40(3), pp. 205-
1160 216.
- 1161 Grabosky, J., Bassuk, N., Irwin, L. & Van Es, H., 1998. *Pilot field study of structural soil*
1162 *materials in pavement profiles*. Champaign, IL, International Society of Arboriculture, pp.
1163 210-221.
- 1164 Grabosky, J., Haffner, E. & Bassuk, N., 2009. Plant available moisture in stone-soil media
1165 for use under pavement while allowing urban tree root growth. *Arboriculture & Urban*
1166 *Forestry*, 35(5), pp. 271-278.
- 1167 Gregory, P. J., 2006. *Plant roots: growth, activity and interaction with soils*. s.l.:Blackwell
1168 Publishing.
- 1169 Gregory, P. J. et al., 2003. Non-invasive imaging of roots with high resolution X-ray micro-
1170 tomography. In: *Roots: the dynamic interface between plants and the Earth*. Dordrecht:
1171 Springer, pp. 351-359.
- 1172 Guo, L. et al., 2013. Application of ground penetrating radar for coarse root detection
1173 and quantification: a review. *Plant and Soil*, Volume 362, pp. 1-23.
- 1174 Hansen, E. M. & Goheen, E. M., 2000. *Phellinus weirii* and other native root pathogens
1175 as determinants of forest structure and process in western North America. *Annual*
1176 *review of phytopathology*, 38(1), pp. 515-539.
- 1177 Hargreaves, C. E., Gregory, P. J. & Bengough, A. G., 2009. Measuring root traits in barley
1178 (*Hordeum vulgare* ssp. *vulgare* and ssp. *spontaneum*) seedlings using gel chambers, soil
1179 sacs and X-ray microtomography. *Plant and Soil*, 316(1-2), pp. 285-297.

- 1180 Heeraman, D. A., Hopmans, J. W. & Clausnitzer, V., 1997. Three dimensional imaging of
1181 plant roots in situ with X-ray computed tomography. *Plant and soil*, 189(2), pp. 167-179.
- 1182 Heeraman, D. A. & Juma, N. G., 1993. A comparison of minirhizotron, core and monolith
1183 methods for quantifying barley (*Hordeum vulgare* L.) and fababean (*Vicia faba* L.) root
1184 distribution. *Plant and Soil*, Volume 148, pp. 29-41.
- 1185 Henwood, K., 1973. A structural model of forces in buttressed tropical rain forest trees.
1186 *Biotropica*, pp. 83-89.
- 1187 Hruska, J., Cermak, J. & Sustek, S., 1999. Mapping tree root systems with ground-
1188 penetrating radar. *Tree Physiology*, Volume 19, pp. 125-130.
- 1189 Huisman, J., Hubbard, S., Redman, J. & Annan, A. P., 2003. Measuring soil water content
1190 with ground penetrating radar: a review. *Vadose Zone Journal*, 2(4), pp. 476-491.
- 1191 Innes, J. L., 1993. *Forest health: its assessment and status*. s.l.: Cab International.
- 1192 Iwase, J. et al., 2015. Non-invasive acoustic sensing of belowground wooden tissues:
1193 possible applications to spatial mapping of soil usage by tree roots. *Environmental*
1194 *Control in Biology*, 53(3), pp. 175-179.
- 1195 Jackson, R. B. et al., 1996. A global analysis of root distributions for terrestrial biomes.
1196 *Oecologia*, pp. 389-411.
- 1197 Jol, H. M. ed., 2008. *Ground penetrating radar theory and applications*. s.l.:Elsevier.
- 1198 Kaestner, A., Schneebeli, M. & Graf, F., 2006. Visualizing three-dimensional root
1199 networks using computed tomography. *Geoderma*, 136(1-2), pp. 459-469.
- 1200 Kearey, P., Brooks, M. & Hill, I., 2013. *An introduction to geophysical exploration*.
1201 s.l.:John Wiley & Sons.
- 1202 Kopinga, J., 1994. *Aspects of the damage to asphalt road pavings caused by tree roots*.
1203 Savoy, IL, International Society of Arboriculture, pp. 165-178.

- 1204 Krainyukov, A. & Lyaksa, I., 2016. Detection of tree roots in an urban area with the use
1205 of ground penetrating radar. *Transport and Telecommunication*, Volume 17, pp. 362-
1206 370.
- 1207 Lambot, S., Javaux, M., Hupet, F. & Vanclooster, M., 2002. A global multilevel coordinate
1208 search procedure for estimating the unsaturated soil hydraulic properties. *Water*
1209 *Resources Research*, 38(11).
- 1210 Lantini, L. et al., 2018. *Use of ground penetrating radar for assessing interconnections*
1211 *between root systems of different matured tree species*. Cassino, Italy, IEEE.
- 1212 Leskovar, D. I., Cantliffe, D. J. & Stoffella, P. J., 1994. Transplant production systems
1213 influence growth and yield of fresh-market tomatoes. *Journal of the American Society*
1214 *for Horticultural Science*, 119(4), pp. 662-668.
- 1215 Liebhold, A. M. et al., 2012. Live plant imports: the major pathway for forest insect and
1216 pathogen invasions of the US. *Frontiers in Ecology and the Environment*, 10(3), pp. 135-
1217 143.
- 1218 Lindsey, P. & Barlow, L., 1994. *The Design of Structural Soil Mixes for Trees in Urban*
1219 *Areas*. s.l.:s.n.
- 1220 Loh, F. C. W., Grabosky, J. & Bassuk, N., 2003. Growth response of *Ficus benjamina* to
1221 limited soil volume and soil dilution in a skeletal soil container study. *Urban Forestry &*
1222 *Urban Greening*, Volume 2, pp. 53-62.
- 1223 Loizos, A. & Plati, C., 2007. Accuracy of ground penetrating radar horn-antenna
1224 technique for sensing pavement subsurface. *IEEE Sensor Journal*, 7(5), pp. 842-850.
- 1225 Loperte, A. et al., 2006. 2D and 3D high resolution geoelectrical tomography for non -
1226 destructive determination of the spatial variability of plant root distribution: laboratory
1227 experiments and field measurements. *Geophysical Research Abstracts*, Volume 8.
- 1228 Lorenzo, H., Pérez - Gracia, V., Novo, A. & Armesto, J., 2010. Forestry applications of
1229 ground - penetrating radar. *Forest Systems*, Volume 19, pp. 5-17.

- 1230 Lucke, T. et al., 2011. *Using permeable pavements to promote street tree health, to*
1231 *minimize pavement damage and to reduce stormwater flows*. Porto Alegre, Brazil, s.n.
- 1232 Lundström, T., Jonsson, M. J. & Kalberer, M., 2007. The root–soil system of Norway
1233 spruce subjected to turning moment: resistance as a function of rotation. *Plant and Soil*,
1234 300(1-2), pp. 35-49.
- 1235 MacLeod, R. D. & Cram, J. W., 1996. *Forces exerted by tree roots*, s.l.: Arboriculture
1236 Research and Information Note-Department of the Environment (United Kingdom).
- 1237 Mahesh, M., 2002. The AAPM/RSNA physics tutorial for residents: search for isotropic
1238 resolution in CT from conventional through multiple-row detector. *Radiographics*, 22(4),
1239 pp. 949-962.
- 1240 Majdi, H., 1996. Root sampling methods - applications and limitations of the
1241 minirhizotron. *Plant and Soil*, Volume 185, pp. 255-258.
- 1242 Majdi, H. et al., 2005. Measuring fine root turnover in forest ecosystems. *Plant and Soil*,
1243 pp. 1-8.
- 1244 Marchi, L. et al., 2018. State of the Art on the Use of Trees as Supports and Anchors in
1245 Forest Operations. *Forests*, 9(8).
- 1246 McPherson, E. G. & Peper, P., 2000. *Costs due to conflicts between street tree root*
1247 *growth and hardscape*. Cohasset, CA, Western Chapter (International Society of
1248 Arboriculture), pp. 15-18.
- 1249 Mooney, S. J., Pridmore, T. P., Helliwell, J. & Bennet, M. J., 2012. Developing X-ray
1250 Computed Tomography to non-invasively image 3-D root systems architecture in soil.
1251 *Plant and Soil*, Volume 352, pp. 1-22.
- 1252 Mullaney, J., Lucke, T. & Trueman, S. J., 2015. A review of benefits and challenges in
1253 growing street trees in paved urban environments. *Landscape and Urban Planning*,
1254 Volume 134, pp. 157-166.

- 1255 Neumann, G., George, T. S. & Plassard, C., 2009. Strategies and methods for studying
1256 the rhizosphere—the plant science toolbox. *Plant and Soil*, 321(1-2), pp. 431-456.
- 1257 Nicoll, B. C. & Armstrong, A., 1998. Development of Prunus root systems in a city street:
1258 Pavement damage and root architecture. *Arboricultural Journal* , pp. 259-270.
- 1259 Nobel, P. S., 2003. *Environmental biology of agaves and cacti*. s.l.:Cambridge University
1260 Press.
- 1261 Ortuani, B., et al., 2013. A non-invasive approach to monitor variability of soil water
1262 content with electromagnetic methods. *Procedia Environmental Sciences*, Volume 19,
1263 pp. 446-455.
- 1264 Ow, L. F. & Sim, E. K., 2012. Detection of urban tree roots with the ground penetrating
1265 radar. *Plant Biosystems*, Volume 146, pp. 288-297.
- 1266 Pallardy, S. G., 2008. *Physiology of Woody Plants*. s.l.:Academic Press.
- 1267 Panissod, C., Michot, D., Benderitter, Y. & Tabbagh, A., 2001. On the effectiveness of 2D
1268 electrical inversion results: an agricultural case study. *Geophysical Prospecting*, Volume
1269 49, pp. 570-576.
- 1270 Patriarca, C., T et al., 2013. Frequency dependent electric properties of homogeneous
1271 multi-phase lossy media in the ground-penetrating radar frequency range. *Journal of*
1272 *Applied Geophysics*, Volume 97, pp. 81-88.
- 1273 Perret, J. S., Al-Belushi, M. E. & Deadman, M., 2007. Non-destructive visualization and
1274 quantification of roots using computed tomography. *Soil Biology and Biochemistry*,
1275 39(2), pp. 391-399.
- 1276 Pokorny, J. D. et al., 2003. *Urban tree risk management: a community guide to program*
1277 *design and implementation*. s.l.:s.n.
- 1278 Potin, D., Duflos, E. & Vanheeghe, P., 2006. Landmines Ground-Penetrating Radar Signal
1279 Enhancement by Digital Filtering. *IEEE Transaction on Geoscience and Remote Sensing*,
1280 Volume 44, pp. 2393-2406.

- 1281 Randrup, T. B., McPherson, E. G. & Costello, L. R., 2001. A review of tree root conflicts
1282 with sidewalks, curbs, and roads. *Urban Ecosystems*, Volume 5, pp. 209-225.
- 1283 Randrup, T. B., McPherson, E. G. & Costello, L. R., 2001. Tree root intrusion in sewer
1284 systems: review of extent and costs. *Journal of Infrastructure System*, pp. 26-31.
- 1285 Richardson, D. M. et al., 2001. Naturalization and invasion of alien plants: concepts and
1286 definitions. *Diversity and Distributions*, 6(2), pp. 93-107.
- 1287 Rishbeth, J., 1972. Resistance to fungal pathogens of tree roots. *Proceedings of the Royal*
1288 *Society of London. Series B. Biological Sciences*, 181(1064), pp. 333-351.
- 1289 Roberts, J., Jackson, N. & Smith, M., 2006. *Tree Roots in the Built Environment*. s.l.:Centre
1290 for Ecology and Hydrology (Great Britain).
- 1291 Samouelian, A. et al., 2005. Electrical resistivity survey in soil science: a review. *Soil &*
1292 *Tillage Research*, Volume 83, pp. 173-193.
- 1293 Samuelson, L. J. et al., 2008. Growth and physiology of loblolly pine in response to long-
1294 term resource management: defining growth potential in the southern United States.
1295 *Canadian Journal of Forest Research*, 38(4), pp. 721-732.
- 1296 Santini, A. et al., 2012. Biogeographical patterns and determinants of invasion by forest
1297 pathogens in Europe. *New Phytologist*.
- 1298 Satriani, A., Loperte, A., Proto, M. & Bavusi, M., 2010. Building damage caused by tree
1299 roots: laboratory experiments of GPR and ERT surveys. *Advances in Geosciences*, pp.
1300 133-137.
- 1301 Schrock, B. J., 1994. *Existing sewer evaluation and rehabilitation*. s.l.:s.n.
- 1302 Schuurman, J. J. & Goedewaagen, M. A. J., 1965. *Methods for the examination of root*
1303 *systems and roots*, s.l.: Wageningen: Centre for agricultural publications and
1304 documentation.

- 1305 Shainsky, L. J. & Radosevich, S. R., 1992. Mechanisms of competition between Douglas-
1306 fir and red alder seedlings. *Ecology*, pp. 30-45.
- 1307 Smit, A. L. et al., 2013. *Root Methods: A Handbook*. s.l.:Springer Science & Business
1308 Media.
- 1309 Stoke, A., 1994. *Response of young trees to wind: effects on root architecture and*
1310 *anchorage strength*, York: s.n.
- 1311 Stokes, A. et al., 2002. An evaluation of different methods to investigate root system
1312 architecture of urban trees in situ: I. Ground-penetrating radar. *Journal of Arboriculture*,
1313 pp. 2-10.
- 1314 Stone, E. L. & Kalisz, P. J., 1991. On the maximum extent of tree roots. *Forest Ecology*
1315 *and Management*, pp. 59-102.
- 1316 Stover, D. B., Day, F. P., Butnor, J. R. & Drake, B. G., 2007. Effect of elevated CO₂ on
1317 coarse-root biomass in Florida scrub detected by ground-penetrating radar. *Ecology*,
1318 88(5).
- 1319 Strong, W. L. & La Roi, G. H., 1983. Root-system morphology of common boreal forest
1320 trees in Alberta, Canada. *Canadian Journal of Forest Research*, pp. 1164-1173.
- 1321 Sullivan, R. H., Gemmell, R. S., Schafer, L. A. & Hurst, W. D., 1977. *Economic analysis,*
1322 *root control, and backwater flow control as related to infiltration/inflow control.*
1323 Cincinnati: s.n.
- 1324 Sustek, S., Hruska, J., M., D. & Michalek, T., 1999. Root surfaces in the large oak tree
1325 estimated by image analysis of the map obtained by the ground penetrating radar.
1326 *Journal of Forest Science*, Volume 45, pp. 139-143.
- 1327 Taylor, H. M., Upchurch, D. R., Brown, J. M. & Rogers, H. H., 1991. Some methods of root
1328 investigations. In: *Developments in Agricultural and Managed Forest Ecology*.
1329 s.l.:Elsevier, pp. 553-564.

- 1330 Tosti, F., Bianchini Ciampoli, L., Brancadoro, M. G. & Alani, A. M., 2018a. GPR
1331 applications in mapping the subsurface root system of street trees with road safety-
1332 critical implications. *Advances in transportation studies*, Volume 44.
- 1333 Tosti, F. et al., 2018b. An experimental-based model for the assessment of the
1334 mechanical properties of road pavements using ground-penetrating radar. *Construction
1335 and Building Materials*, Volume 165, pp. 966-974.
- 1336 Tosti, F. et al., 2016. GPR analysis of clayey soil behaviour in unsaturated conditions for
1337 pavement engineering and geoscience applications. *Near Surface Geophysics*, Volume
1338 14 (2), pp. 127-144.
- 1339 Tosti, F. & Pajewski, L., 2015. Applications of Radar Systems in Planetary Sciences: An
1340 Overview. In: *Civil Engineering Applications of Ground Penetrating Radar*. s.l.:Springer
1341 Transactions in Civil and Environmental Engineering, pp. 361-371.
- 1342 Tracy, S. R., Black, C. R., Roberts, J. A. & Mooney, S. J., 2011. Soil compaction: a review
1343 of past and present techniques for investigating effects on root growth. *Journal of the
1344 Science of Food and Agriculture*, Volume 91, pp. 1528-1537.
- 1345 Tracy, S. R. et al., 2010. The X-factor: visualizing undisturbed root architecture in soils
1346 using X-ray computed tomography. *Journal of Experimental Botany*, 61(2), pp. 311-313.
- 1347 Trowbridge, P. J. & Bassuk, N. L., 2004. *Trees in the Urban Landscape: Site Assessment,
1348 Design, and Installation*. Hoboken, NJ: Wiley.
- 1349 Tubbs, C. H., 1977. *Root-crown relations of young sugar maple and yellow birch*, s.l.: s.n.
- 1350 Wagar, J. A. & Barker, P. A., 1983. Tree root damage to sidewalks and curbs. *Journal of
1351 Arboriculture*, Volume 9, pp. 177-181.
- 1352 Wagar, J. A. & Franklin, A. L., 1994. Sidewalk effects on soil moisture and temperature.
1353 *Journal of Arboriculture*, Volume 20, pp. 237-238.
- 1354 Wang, X., Allison, R. B., Wang, L. & Ross, R. J., 2007. *Acoustic tomography for decay
1355 detection in red oak trees*, Madison, WI: United States Department of Agriculture.

- 1356 Wang, Z. et al., 2006. Fine root architecture, morphology, and biomass of different
1357 branch orders of two Chinese temperate tree species. *Plant and Soil*, pp. 155-171.
- 1358 Weaver, J. E. & Voigt, J., 1950. Monolith Method of Root-Sampling in Studies on
1359 Succession and Degeneration. *Agronomy & Horticulture - Faculty Publications*.
- 1360 Wielopolski, L., Hendrey, G., Daniels, J. & McGuigan, M., 2000. *Imaging Tree Root*
1361 *Systems In Situ*. s.l., s.n., pp. 642-646.
- 1362 Wildenschild, D. et al., 2002. Using X-ray computed tomography in hydrology: systems,
1363 resolutions, and limitations. *Journal of Hydrology*, Volume 267, pp. 285-297.
- 1364 Williams, R. E., Shaw, C. G., Wargo, P. M. & Sites, W. H., 1986. *Armillaria root disease*.
1365 s.l.:US Department of Agriculture, Forest Service.
- 1366 Wilson, B. F., 1964. *Structure and growth of woody roots of Acer rubrum L.* s.l.:Harvard
1367 University, Harvard Forest.
- 1368 Zenone, T. et al., 2008. Preliminary use of ground-penetrating radar and electrical
1369 resistivity tomography to study tree roots in pine forests and poplar plantations.
1370 *Functional Plant Biology*, Volume 35, pp. 1047-1058.
- 1371